

# Solving the 3D Ising model with conformal bootstraps

Loos E., Ottens C., Van Vliet P.

May 2018

# Contents

<b>1</b>	<b>Introduction</b>	<b>3</b>
<b>2</b>	<b>The Conformal Bootstrap Philosophy</b>	<b>4</b>
2.1	The origin of the bootstrap . . . . .	4
2.2	The Bootstrap equations . . . . .	5
2.3	The geometrical approach . . . . .	7
<b>3</b>	<b>Solving the 2D Ising model</b>	<b>8</b>
3.1	Using the Virasoro algebra to obtain minimal models . . . . .	8
3.2	The minimal model $\mathcal{M}(4,3)$ . . . . .	11
3.3	Solving the 2D Ising model using the geometrical approach . . . . .	12
<b>4</b>	<b>Operators and their dimensions in the 3D Ising model</b>	<b>12</b>
4.1	Bootstrapping vs $\epsilon$ -expansion . . . . .	13
4.2	Ising operators . . . . .	14
<b>5</b>	<b>Solving the 3D Ising model</b>	<b>16</b>
5.1	The conformal bootstrap for $\langle\sigma\sigma\sigma\sigma\rangle$ . . . . .	16
5.2	Method of confining the operator dimension spectrum . . . . .	17
5.3	Results . . . . .	19
5.3.1	Bounds on $\Delta_\epsilon$ . . . . .	19
5.3.2	Bounds on $\Delta_\epsilon$ assuming a gap between $\Delta_\epsilon$ and $\Delta_{\epsilon'}$ . . . . .	20
5.3.3	Bounds on the gap in the spin 2 sector . . . . .	22
<b>6</b>	<b>Outlook</b>	<b>23</b>
<b>A</b>	<b>Some basic Conformal Field Theory</b>	<b>25</b>
A.1	Scale and Weyl invariance . . . . .	25
A.2	Conformal invariance . . . . .	26
<b>B</b>	<b>Recursion relations for conformal blocks</b>	<b>29</b>
<b>C</b>	<b>Conformal blocks of spin 0 and 1</b>	<b>31</b>
<b>D</b>	<b>Recursion relation <math>h_{m,n}</math></b>	<b>33</b>

# 1 Introduction

In 1944 Onsager solved the 2D Ising model on the lattice exactly, for any temperature. This has so far not been done for the 3D model, although it has been attempted by many. Attempts to solve the 3D Ising model at the critical point,  $T = T_c$ , where it shows a second order phase transition (the magnetic susceptibility changes discontinuously) have been more successful. Second order phase transitions are important in liquid-vapor transitions and transitions in binary fluids and uniaxial magnets. The second order phase transition of the Ising model is in the same universality class as those phase transitions [19], so solving the 3D Ising model at the critical point will hopefully give more understanding of second order phase transitions in general. First we introduce the conformal bootstrap and discuss the solution for the 2D Ising model. Then we will review the paper [19] by El-Showk et al. who have tried to solve the 3D Ising model at the critical point in the continuum limit using conformal bootstrapping techniques.

The region close to the critical point has the advantage that the physics is universal and does not depend on the action that is chosen; for example an action with specific nearest-neighbour interactions. At points far away from  $T = T_c$  the choice of action does play a role [17]. Going to the continuum limit means that the lattice spacing goes to zero or equivalently going to large length scales such that the lattice spacing is very small compared to the length scale. This means going to the low energy (IR) limit, where the effects coming from the lattice disappear. At the critical point the correlation length  $\xi(T) \rightarrow \infty$  for  $T \rightarrow T_c$ . We see that in this limit, the two-point function of the spin operator changes form [17]:

$$\langle \sigma(0)\sigma(r) \rangle \sim e^{-r/\xi(T)} \xrightarrow{T \rightarrow T_c, \xi \rightarrow \infty} \langle \sigma(0)\sigma(r) \rangle \frac{1}{|r|^{2\Delta}} (T = T_c)$$

The exponent which had a length scale in it vanishes and the model becomes invariant under scale transformations. The two-point function has a power-law form at the critical point. In 2D, Zamolodchov and Polchinski have shown [11, 21] that scale invariance also implies conformal invariance, so the 2D Ising model is a conformal theory at the critical point. In 3D this is not proven yet, but it looks like this is the case and conformal invariance seems to be present at critical points [19]. We will assume, as they did in [19], that at the critical point, the 3D Ising model is also conformally invariant.

With this assumption, El-Showk et al. have tried to find bounds on the operator dimensions of the 3D Ising model, using conformal bootstrap techniques [19]. In this article we will rederive their outcomes and explain the results they found and their impact. We will assume a basic level of knowledge of Conformal Field Theory (CFT). An overview is given in appendix A.

In section 2 we will explain the conformal bootstrap and the philosophy behind it. In section 3 we will discuss the success of solving the 2D Ising model at the critical point using the same conformal bootstrap techniques.

In section 4 we will have a closer look at the lowest dimensional operators of the 3D Ising model and in section 5 we will use the conformal bootstrap to obtain bounds on the dimensions of the three lowest dimensional operators. Sections 4 and 5 closely follow [19] and aim to rederive and explain their results.

## 2 The Conformal Bootstrap Philosophy

### 2.1 The origin of the bootstrap

In the 1960s particle physics took a great flight and physicists tried to divide newfound particles in fundamental building blocks and composites. Geoffrey Chew was against such a method as “Nature is as it is because it is the only possible consistent Nature”. He claimed he could find Nature’s laws just from self-consistency conditions, by “pulling them up from their own bootstraps” [20]. In particle physics this method fell into oblivion, but it came to use in Conformal Field Theory (CFT).

We can see Quantum Field Theories (QFTs) as a renormalization group (RG) flow between conformal points: a flow between a CFT in the UV and the IR. Classifying the CFTs would give a framework in which all the QFTs live. The conformal bootstrap is a way to classify CFTs.

The idea of the conformal bootstrap was first suggested in the 1970s by Polyakov [13]. Until then the way to describe strong interactions in QFT was to solve part of the problem (the microscopic case) with perturbation on a local action, but this proved to be very difficult. Polyakov solved the 2D Ising model using conformal bootstrap techniques. However, it turned out that solving CFTs using bootstraps in higher dimensions was difficult, but progress has been made in 2008. Rattazzi and Rychkov wondered if the mass inducing we now know comes from the Higgs boson could come from a 4D CFT. This was the start of a lot of progress in the bootstrap region. How does CFT correspond to other problems? The 3D Ising model becomes conformally invariant at large distances. But this IR CFT is the same CFT that arises from the  $\phi^4$  theory or the critical point of water at its phase diagram. The same IR CFT can arise from different microscopic systems. This means these theories are *IR equivalent* at their critical points. This is also called *critical universality*. This means that we can study the CFT by doing computations in any of the microscopic theories. But another powerful tool is using the IR-symmetries arising at the critical points. This leads to the Conformal Bootstrap:

1. Focus on the CFT and not on one of its microscopic realizations.
2. Determine the consequences of the conformal symmetries.
3. Impose consistency conditions on the theory.
4. Use this to constrain and (if possible) solve the theory.

## 2.2 The Bootstrap equations

Under the Operator Product Expansion (OPE) the primary operators of a CFT form an algebra. The OPE allows us to express the product of two local quantum fields in terms of well-defined local fields,

$$\phi_i(x)\phi_j(y) = \sum_{\mathcal{O}} f_{ij\mathcal{O}} C_{ij}^{\mathcal{O}}(x-y, \partial_y) \mathcal{O}(y), \quad (1)$$

where we sum over all primaries, the  $C_{ij}^{\mathcal{O}}$  are analytic differential operators that are fixed by conformal invariance. The  $f_{ij\mathcal{O}}$  are the OPE coefficients. If we know the OPE coefficients  $f_{ij\mathcal{O}}$ , the spins,  $l$ , and the operator dimensions of the primary operators  $\Delta_{\mathcal{O}}$ , we know the complete operator algebra of conformal fields. These numbers comprise the ‘‘CFT data’’.

Computing  $n$ -point functions seems like a hard task, but it is possible to express  $n$ -point functions in terms of three-point functions. Conformal symmetry severely constrains the correlation functions of local operators. A two-point function for scalars generally looks like,

$$\langle \mathcal{O}(x)\mathcal{O}(y) \rangle = \frac{1}{|x-y|^{2\Delta_{\mathcal{O}}}}.$$

And three-point functions,

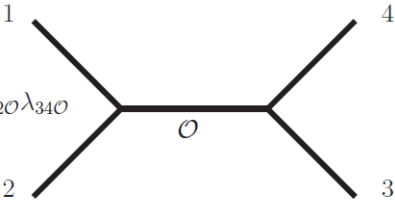
$$\langle \mathcal{A}(x)\mathcal{B}(y)\mathcal{C}(z) \rangle = \frac{f_{ABC}}{|x-y|^{\Delta_{\mathcal{A}}+\Delta_{\mathcal{B}}-\Delta_{\mathcal{C}}}|y-z|^{\Delta_{\mathcal{B}}+\Delta_{\mathcal{C}}-\Delta_{\mathcal{A}}}|z-x|^{\Delta_{\mathcal{C}}+\Delta_{\mathcal{A}}-\Delta_{\mathcal{B}}}},$$

with  $\Delta_{\mathcal{O}}$  the scaling dimension of  $\mathcal{O}(x)$ . The  $f_{ABC}$  are the three-point coefficients (we can identify these with the OPE coefficients from (1)). These coefficients are normalized to be 1 for two-point functions ( $\langle \Delta|\Delta \rangle = 1$ ). For higher dimensions we do not have this freedom anymore. Surprisingly we do not need explicit expressions for higher-point functions than three-point functions. In the 1970s among others Polyakov [13] discovered a way to express higher-point functions in terms of two-point functions. This is called the *conformal block decomposition*. Using expansion (1) this gives for a four-point function of scalar operators,

$$\langle \phi_1\phi_2\phi_3\phi_4 \rangle = \sum_{\mathcal{O}} f_{12\mathcal{O}} f_{34\mathcal{O}} C_{34}^{\mathcal{O}} C_{12}^{\mathcal{O}} \langle \mathcal{O}(x)\mathcal{O}(y) \rangle \quad (2)$$

$$= \sum_{\mathcal{O}} \frac{f_{12\mathcal{O}} f_{34\mathcal{O}} G_{\Delta,l}(u,v)}{(x_{12}^2)^{\frac{1}{2}(\Delta_1+\Delta_2)} (x_{34}^2)^{\frac{1}{2}(\Delta_3+\Delta_4)} \left(\frac{x_{24}^2}{x_{14}^2}\right)^{\frac{1}{2}\Delta_{12}} \left(\frac{x_{14}^2}{x_{13}^2}\right)^{\frac{1}{2}\Delta_{34}}} \quad (3)$$

or schematically (figure from [15], the  $f_{ij\mathcal{O}}$  are here  $\lambda_{ij\mathcal{O}}$ ),

$$\langle \phi_1(x_1)\phi_2(x_2)\phi_3(x_3)\phi_4(x_4) \rangle = \sum_{\mathcal{O}} \lambda_{12\mathcal{O}} \lambda_{34\mathcal{O}}$$


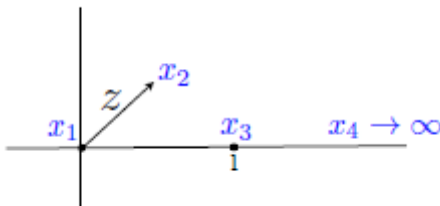


Figure 1: We can place the four points on the plane in this way using conformal invariance. This leaves two coordinates free. Source: [6].

In equation (3)  $u$  and  $v$  are the conformally invariant cross-ratios:

$$u = \frac{x_{12}^2 x_{23}^2}{x_{13}^2 x_{24}^2}, \quad v = \frac{x_{14}^2 x_{23}^2}{x_{13}^2 x_{24}^2}. \quad (4)$$

Conformal invariance ensures there are exactly two undetermined quantities. How? Using special conformal transformations we can put one term ( $x_4$ ) on infinity. We set  $x_1$  to zero using translations. Using rotations and dilatations we fix  $x_3$  on  $(1, 0, 0, 0)$ . Now three points are on one line and  $x_2$  is at position  $z$  in the complex plane (see figure 1).

The  $G_{\Delta,l}(u, v)$  are the *conformal blocks*. But this shows an ambiguity. Instead of gluing together  $\phi_1$  with  $\phi_2$  we could also have taken  $\phi_1$  with  $\phi_4$ ; we could have chosen a different OPE channel (14)(23) instead of (12)(34). To make the CFT consistent these three-channels should be the same:

$$\sum_{\mathcal{O}} \lambda_{12\mathcal{O}} \lambda_{34\mathcal{O}} \quad \begin{array}{c} 1 \\ \diagdown \\ \text{---} \mathcal{O} \text{---} \\ \diagup \\ 2 \end{array} \quad \begin{array}{c} 4 \\ \diagup \\ \text{---} \\ \diagdown \\ 3 \end{array} = \sum_{\mathcal{O}'} \lambda_{14\mathcal{O}'} \lambda_{23\mathcal{O}'} \quad \begin{array}{c} 1 \\ \diagdown \\ \text{---} \mathcal{O}' \text{---} \\ \diagup \\ 2 \end{array} \quad \begin{array}{c} 4 \\ \diagup \\ \text{---} \\ \diagdown \\ 3 \end{array}$$

This is the *Bootstrap condition*, also called OPE associativity (it shows the associativity of the operator algebra) or crossing symmetry. This imposes a constraint on the OPE coefficients of the form

$$\sum_{\mathcal{O}} f_{12\mathcal{O}} f_{34\mathcal{O}}(\dots) = \sum_{\mathcal{O}'} f_{14\mathcal{O}'} f_{23\mathcal{O}'}(\dots). \quad (5)$$

Because we can express  $n$ -point functions in terms of  $n - 1$ -point functions it is enough to have crossing symmetry on four-pointfunctions. No additional constraints on higher point functions are needed. This is shown in Figure 2. This constraint is necessary and sufficient to define a consistent CFT. Using this to classify CFT's and their properties is called the Conformal Bootstrap approach.

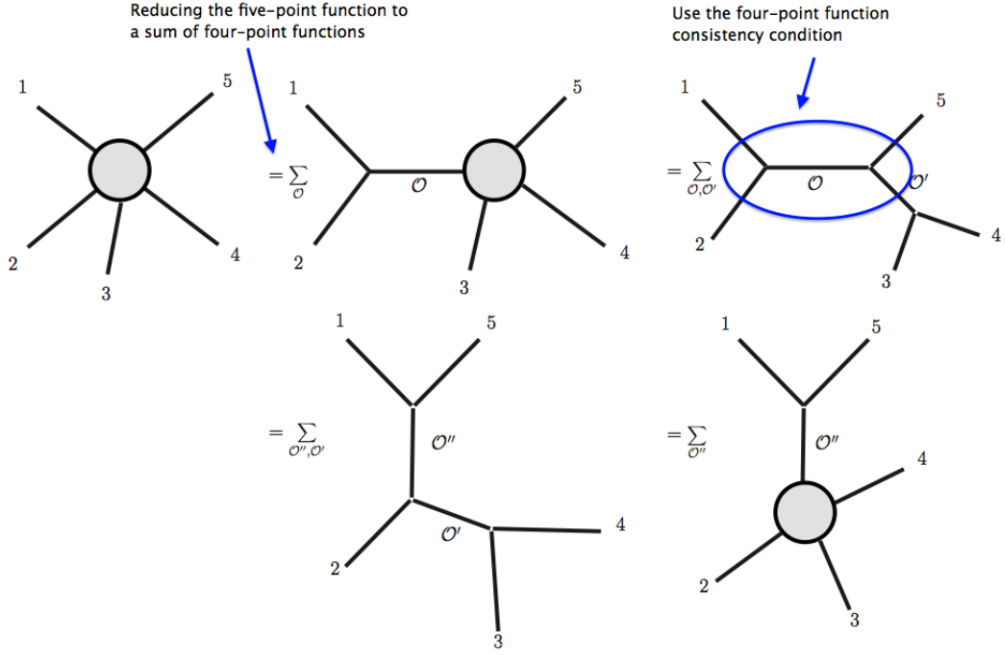


Figure 2: This shows that no additional crossing symmetries are needed by example of a five-point function. The (12) and (15) channels should be the same. Source: [15].

In this article we will focus on solving the Ising model with the conformal bootstrap. The scaling dimensions in the CFT data are directly related to the critical exponents used in this model. The scaling dimension of the energy operator  $\epsilon$  for example gives the exponent  $\nu$  describing the correlation length  $\xi$  when approaching the critical temperature  $T_c$  [10],

$$\xi \propto |T - T_c|^{-\nu},$$

$$\nu = \frac{1}{3 - \Delta_\epsilon},$$

and combined with the scaling dimension  $\Delta_\sigma$  of the spin operator it gives the exponent  $\gamma$  related to the susceptibility  $\chi$ ,

$$\chi \propto |T - T_c|^{-\gamma},$$

$$\gamma = \frac{3 - 2\Delta_\sigma}{3 - \Delta_\epsilon}.$$

In section 4 the 3D Ising operators are discussed in greater detail.

### 2.3 The geometrical approach

When the crossing equation (5) was suggested Belavin et al. [1] used it to solve the 2D Ising model. But it has proved to be difficult to solve for higher dimensional CFTs. In 2008 Rattazzi, Rychkov, Tonni, and Vichi approached the problem geometrically and tried to narrow the set of CFTs by deriving

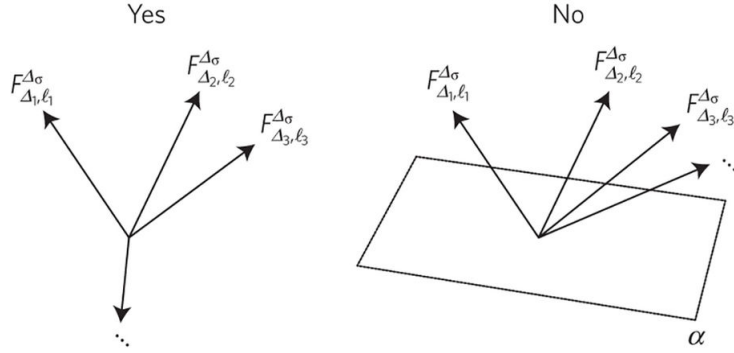


Figure 3: The sum of functions. On the right a separating plane  $\alpha$  can be found and these dimensions can be excluded. Source: [10].

bounds on the CFT data. This is a general approach that theoretically can be used in all higher-dimensional CFTs, in section 5 this is done for the 3D Ising model CFT.

If we compute the four-point function for four identical operators, for example the spin operator, we get conformal blocks for the same operator and 3 and 5 together give a constraint of the form,

$$\sum_{\Delta, l} f_{\sigma\sigma\mathcal{O}}^2 \mathbf{F}_{\Delta, l}^{\Delta_\sigma} = 0. \quad (6)$$

Now we can consider the  $\mathbf{F}_{\Delta, l}^{\Delta_\sigma}$  as vectors in the functionspace of four points. Equation (6) tells us that the vectors must sum to zero, even though they have positive coefficients. In Figure 3 this is shown. If we can find a separating plane such that all the vectors are on one side of it, this constraint cannot be fulfilled. Thus the set  $\{(\Delta_1, l_1), (\Delta_2, \dots)\}$  can be excluded as possible CFT data. It suffices to consider a finite-dimensional subspace even though the function space is infinite-dimensional. If not all the possible scaling dimensions and spins are known, choose the unknown dimensions and spins such that the  $\mathbf{F}_{\Delta, l}^{\Delta_\sigma}$  lie on one side of the plane. In the Ising model for example we search for  $\Delta_\sigma$  and  $\Delta_\epsilon$ . Fix values for  $(\Delta_\sigma, \Delta_\epsilon)$  and search for a separating plane. If this is found, these dimensions can be excluded.

### 3 Solving the 2D Ising model

In 1970 Polyakov proposed conformal invariance of critical fluctuations [12]. Then the conformal bootstrap could be used to solve critical point theories, and he did so in 1984 for the 2D Ising model. We will outline his method in [1] to solve the 2D conformal bootstrap exactly and then comment on the geometrical approach from 2.3.

#### 3.1 Using the Virasoro algebra to obtain minimal models

The difference in 2D with higher dimensional CFTs is that the Virasoro algebra can be used.



The conformal transformations are generated by the algebra of differential operators  $l_n = z^{n+1} \frac{d}{dz}$  which satisfy the commutation relations  $[l_n, l_m] = (n - m)l_{n+m}$ . The extension of this algebra is the Virasoro algebra  $\mathcal{L}_c$ , defined by the commutation relations,

$$[L_n, L_m] = (n - m)L_{n+m} + \frac{1}{12}c(n^3 - n)\delta_{n+m,0}. \quad (7)$$

These are the mode-operators of the energy-momentum tensor. The Virasoro algebra contains a subalgebra  $SL(2, \mathbb{C})$  generated by  $L_0, L_1$  and  $L_{-1}$ . This is the algebra of special conformal translations. The representation space of the conformal algebra is given by the Verma module  $V_n$ . Each conformal family  $[\phi]$  (primary and its descendants) corresponds to a representation.

The Virasoro algebra plays a very important role. The Bootstrap equation (5) can be solved in a few special cases because the conformal blocks can be computed exactly. This happens for certain dimensions  $\Delta$  associated with the degenerate representation of the Virasoro algebra.

The Verma module  $V_\Delta$  is irreducible unless it contains a nullvector (also called the *highest weight state*  $|\chi\rangle$ ) satisfying,

$$\begin{aligned} L_n |\chi\rangle &= 0 \\ L_0 |\chi\rangle &= (\Delta + K) |\chi\rangle, \end{aligned} \quad (8)$$

with  $K \in \mathbb{N}$ . To obtain the irreducible representation the nullvector  $|\chi\rangle$  must be put to 0. The dimensions for which we can find such a  $|\chi\rangle$  were listed by Kac [9]:

$$\Delta_{(n,m)} = \Delta_0 + \left(\frac{1}{2}\alpha_+ n + \frac{1}{2}\alpha_- m\right)^2, \quad (9)$$

$$\Delta_0 = \frac{1}{24}(c - 1), \quad (10)$$

$$\alpha_\pm = \frac{\sqrt{1 - c} \pm \sqrt{25 - c}}{\sqrt{24}}, \quad (11)$$

where  $c$  is the central charge.

What does this imply for the CFT? With the operator-state correspondence there exists a field with dimension  $\Delta_{(n,m)} + K$  associated to the nullvector  $|\chi\rangle$ . This field is at the same time a primary (because it satisfies equation (8)) and a secondary, as it is a descendant of the field with dimension  $\Delta_{(n,m)}$ . Because it has primary properties we can also consider the tower of descendants of the field  $\phi_{\Delta_{(n,m)}+K}$ . These are all zero with eq. (8) and removing these fields from the conformal family  $[\phi_{\Delta_{(n,m)}}]$  gives the irreducible conformal family (the *degenerate conformal family*). This contains less fields than it normally would, it is truncated. A useful property of these conformal families is that its correlation functions satisfy linear partial differential equations [1, 7]. This imposes constraints on the operator algebra and enables us to find the conformal blocks. CFTs containing only degenerate conformal families are called *minimal models*. They are characterised by a

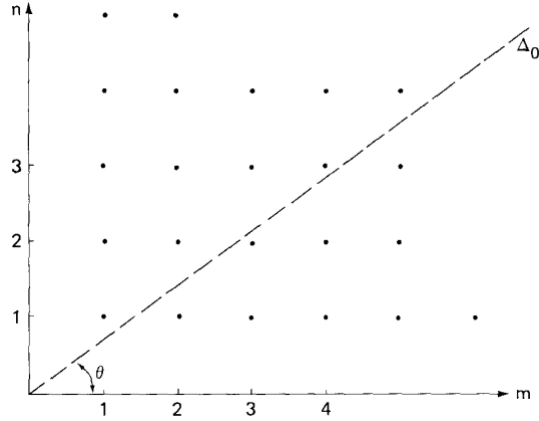


Figure 4: Diagram of dimensions. The dots represent the allowed dimensions, listed by  $n, m$ . Source: [7].

*finite* amount of representations. More details can be found in [7].

Let us go back to the Kac formula (9) and see what it tells us about the allowed dimensions. Three sectors can be identified. For  $c \geq 25$  the  $\alpha_{\pm}$  are complex thus the second term becomes negative. For  $n, m$  sufficiently large  $\Delta_{(n,m)}$  becomes negative and does not satisfy the unitarity bound. The second sector comprises  $1 \leq c < 25$ . Then only one term of  $\alpha_{\pm}$  is complex and the scaling dimension becomes complex. So to get physical dimensions we narrow our attention to the sector  $0 < c \leq 1$ . We can present the allowed dimensions in a “diagram of dimensions” (see Figure 4). The baseline is given by  $\Delta_0$  and the allowed dimensions can be represented by dots in a plane. The angle between  $\Delta_0$  and these dots is given by the ratio  $\tan(\theta) = -\frac{\alpha_-}{\alpha_+} = \frac{\sqrt{25-c}-\sqrt{1-c}}{\sqrt{25-c}+\sqrt{1-c}} = \frac{p}{q}$ .

In [7, 1] *fusion rules* are worked out. These rules show which conformal families occur in the OPE of two fields. According to fusion rules we not only get truncation from below as we described earlier, but also from above. These rules imply that the degenerate fields with  $n \geq p$  or  $m \geq q$  drop out. After truncation from fusion rules the theory only contains the families associated with the dots inside the rectangle enclosed by  $p$  and  $q$ . This severely constrains the conformal families in the theory and the allowed dimensions. A minimal model is characterised by  $\mathcal{M}(q, p)$ . From the rectangle and integer spacing of the operators it is clear that there are  $\frac{1}{2}(p-1)(q-1)$  allowed dimensions. The 2D Ising model coincides with the minimal model  $\mathcal{M}(4, 3)$ . This minimal model also describes the free theory of a Majorana fermion.

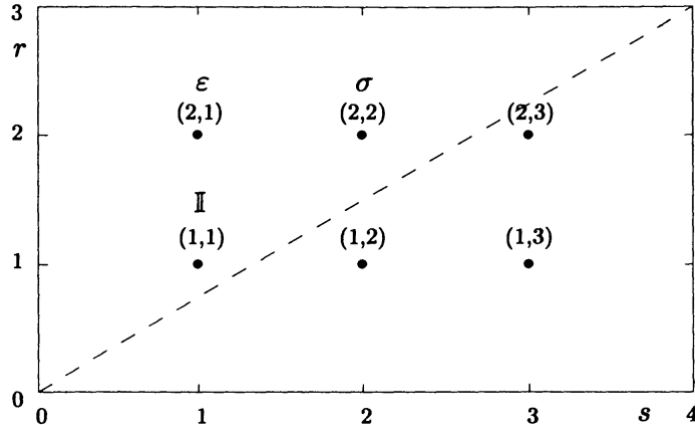


Figure 5: Diagram of dimensions for the minimal model  $\mathcal{M}(4,3)$  with central charge  $c = \frac{1}{2}$ . Only the allowed 6 dimensions inside the rectangle are shown. Source: [1].

### 3.2 The minimal model $\mathcal{M}(4,3)$

We start from the central charge  $c = \frac{1}{2}$ . This gives the minimal model  $\mathcal{M}(4,3)$ . Computing (9) for the case at hand yields the dimensions:

$$\begin{aligned} \Delta_{(1,1)} &= \Delta_{(2,3)} = 0 \\ \Delta_{(2,2)} &= \Delta_{(1,2)} = \frac{1}{16}, \end{aligned} \tag{12}$$

$$\Delta_{(2,1)} = \Delta_{(1,3)} = \frac{1}{2}, \tag{13}$$

shown in Figure 5. These dimensions correspond to three degenerate fields, which we can immediately link with the operator-field correspondence to the known identity operator, spin operator and energy operator:

$$\begin{aligned} \psi_{(1,1)} &= \psi_{(2,3)} = \mathbb{I}, \\ \psi_{(2,2)} &= \psi_{(1,2)} = \sigma, \\ \psi_{(2,1)} &= \psi_{(1,3)} = \epsilon. \end{aligned}$$

This theory has the following fusion rules:

$$\begin{aligned} \sigma \times \sigma &= \mathbb{I} + \epsilon, \\ \epsilon \times \sigma &= \sigma, \\ \epsilon \times \epsilon &= \mathbb{I}, \end{aligned}$$

leaving out the trivial fusion rules with the identity. An appropriate set of fields to describe the closed operator algebra is now  $\{\mathbb{I}, \sigma, \epsilon, +\text{descendants}\}$ . To get the full dimensions of the operators  $\sigma$  and  $\epsilon$  we have to add the dimensions in (12) and (13) to get the well-known dimensions  $\Delta_\sigma = \frac{1}{8}$  and  $\Delta_\epsilon = 1$ .

### 3.3 Solving the 2D Ising model using the geometrical approach

In the last subsection we used knowledge of minimal models in CFT to solve the 2D Ising CFT exactly. But the general geometrical approach described in section 2.3 can also be used to derive bounds on the operator dimensions of the 2D Ising CFT, this is done in [14]. Instead of working with the Virasoro algebra we now need to define primaries in  $Sl(2, \mathbb{C})$ . This is achieved by decomposing the Verma module into irreducible  $Sl(2, \mathbb{C})$  representations. An advantage in 2D above 3D is that the conformal blocks are known exactly. These are given by,

$$g_{\Delta,l}(u,v) = \frac{(-)^l}{2^l} [f_{\Delta+l}(z)f_{\Delta-l}(\bar{z}) + (z \leftrightarrow \bar{z})]. \quad (14)$$

The bounds on the operator dimensions from solving equations (6) give a kink very close to  $(\Delta_\sigma = \frac{1}{8}, \Delta_\epsilon = 1)$ . This suggests it is a reasonable method to solve conformal bootstraps and determine the critical dimensions and operator spectrum for the Ising model. This is good news for higher dimensional Ising models which are not exactly solvable.

## 4 Operators and their dimensions in the 3D Ising model

The 3D Ising model is completely known at the critical point in the continuum limit if we know all the dimensions of all the operators and their OPE coefficients. So we are looking for the spectrum of operator dimensions. In a CFT, we can divide the operators in two classes: the primaries and the descendants (see also appendix A). The 3D Ising model has in principle an infinite amount of primary operators and descendants. However, in the literature only seven of the primary operators have been studied. Those seven can be found in Table 1 in [19]. We repeat the table here for convenience.

Operators	Spin $l$	$\mathbb{Z}_2$	$\Delta$	Exponent
$\sigma$	0	-	0.5182(3)	$\Delta = 1/2 + \eta/2$
$\sigma'$	0	-	$\geq 4.5$	$\Delta = 3 + \omega_A$
$\epsilon$	0	+	1.413(1)	$\Delta = 3 - 1/\nu$
$\epsilon'$	0	+	3.84(4)	$\Delta = 3 + \omega$
$\epsilon''$	0	+	4.67(11)	$\Delta = 3 + \omega_2$
$T_{\mu\nu}$	2	+	3	n/a
$C_{\mu\nu\kappa\lambda}$	4	+	5.0208(12)	$\Delta = 3 + \omega_{NR}$

Table 1: Notable low-lying operators of the 3D Ising model at criticality. Source: [19]

Their dimensions as given in Table 1 have been calculated using various techniques, such as Monte Carlo simulations and the  $\epsilon$ -expansion. The last one is the most commonly used one and we will review it here shortly. Then



Figure 6: Renormalization Group flow between two fixed points, which are often found to be conformally invariant. Source: [17].

we will have a look at each of the seven operators individually, to see what role they play. Most of the information in this section comes from a lecture given by Slava Rychkov at CERN in 2013. Video recordings of this lecture can be found online. [17]

#### 4.1 Bootstrapping vs $\epsilon$ -expansion

The  $\epsilon$ -expansion is based on the renormalization group (RG) method, where you start with a free scalar theory that you can perturb by the relevant,  $\mathbb{Z}_2$  preserving operators  $m^2\phi^2 + \lambda\phi^4$ . Relevant in a three-dimensional theory means that the coupling has a positive mass dimension and the operator is relevant at low energies. Note that in  $D = 3$ ,  $[\phi] = \frac{1}{2}$ . From the free scalar theory with a relevant perturbation at the UV we flow to the critical point at the IR (see Figure 6). Along the way, some operators might pick up an anomalous dimension due to quantum loop effects. The problem of this method is that in three dimensions, the region close to the critical point is strongly coupled, so there perturbation theory breaks down and we don't know how to calculate the flow and the anomalous dimensions. The solution to this is to perform a trick. We go to  $D = 4 - \epsilon$ , where this region becomes weakly coupled. The interaction term  $\lambda\phi^4$  is marginal in  $D = 4$ , meaning that  $[\lambda] = 0$ , and we can do normal perturbation theory again. So we compute all the operator dimensions and OPE coefficients in  $4 - \epsilon$  dimensions and express it in a power series in  $\epsilon$ . Then we set  $\epsilon \rightarrow 1$  to get back to  $D = 3$ .

This seems like a valid method. However, the power series in  $\epsilon$  is divergent and the problems already start at the second/third term in the expansion. And with  $\epsilon$  of  $\mathcal{O}(1)$ , perturbation theory cannot be trusted here as well. There are some techniques such as Borel resummation, that can partly solve this problem, but it is still a bit awkward and the calculation of higher dimensional operators becomes imprecise quite quickly. Another thing is that by using this method, or any RG method, we completely throw away the fact that the theory (possibly) has conformal invariance at the critical point. Along the RG flow, conformal invariance is only present at the fixed points, but not along the flow. It feels a bit unsatisfactory to just throw out

something as universal as conformal invariance. Or, as Rychkov put it [17]: “If we are trying to describe something as beautiful and universal, why do we have to do it by trying to arrive at this universal object by flowing through some mud?”. We might want to look for a method that actually exploits the features given by conformal invariance. The conformal bootstrap is such a method.

## 4.2 Ising operators

El-Showk et al. [19] tried to find the operator dimensions using the conformal bootstrap. The values for the dimensions given in Table 1 were used as guidance to see if the bootstrap will reproduce the results found by using other techniques. Let us have a closer look at those operators first. The 3D Ising model on the lattice has global  $\mathbb{Z}_2$  symmetry: the Ising spin flip. This means that all the operators are either odd or even under this symmetry. All the operators considered here are primaries and do not contain derivatives.

The  $\mathbb{Z}_2$  odd operators in the table are  $\sigma$  and  $\sigma'$ . In terms of renormalization group methods, they correspond to  $\phi$  and  $\phi^3$  respectively in the UV theory. While flowing down to the IR, the fields acquire an anomalous dimension and become  $\sigma$  and  $\sigma'$ .  $\sigma$  is the spin operator in the Ising model. The anomalous dimension it acquires is small, of order  $\mathcal{O}(\epsilon^2)$  in the  $\epsilon$ -expansion (the term linear in  $\epsilon$  vanishes). This can also be seen when considering the dimension of  $\sigma$ . It is slightly above  $\frac{1}{2}$ , which is the dimension of  $\phi$  in the 3D free theory. For  $\sigma$  the calculated dimension is accurate, but for  $\sigma'$  this is not the case.  $\sigma'$  is an irrelevant operator in  $D = 3$  ( $\Delta_{\sigma'} > 3$ ) and the  $\epsilon$ -expansion becomes divergent for  $\epsilon \rightarrow 1$  already after the first few terms.

Let us investigate the  $\mathbb{Z}_2$  even operators. The first one is  $\epsilon$ , which is the product of two spins next to each other ( $\sigma_i \sigma_j$ ). It is interpreted as the energy density field. It is the lowest dimensional and only relevant  $\mathbb{Z}_2$  even scalar field. In the UV free theory it corresponds to  $\phi^2$ . Just as the  $\sigma$  operator, also  $\phi^2$ , which has dimension  $\Delta_{\phi^2} = 1$ , will acquire an anomalous dimension when flowing down to the IR and result in the operator  $\epsilon$ . However, the anomalous dimension is not small. As can be seen in Table 1, the anomalous dimension of  $\epsilon$  is  $\omega \approx 0.4$ . This means that the RG flow is strongly coupled and perturbation theory will break down quickly.

$\epsilon'$  is already irrelevant in  $D = 3$  since  $\Delta_{\epsilon'} > 3$ . We can link  $\epsilon'$  to  $\phi^4$  in the UV free theory.  $\phi^4$  is a relevant operator in the free theory, but it will acquire an anomalous dimension which is so large that the operator  $\epsilon'$  is not relevant anymore.  $\epsilon'$  describes the correction to scaling. A long distance correlation function is almost given by the dimension that the conformal field theory predicts, but not quite. It is disturbed by irrelevant operators that get mixed into the Lagrangian, which is a result from lattice effects. This admixture is small, but present. Of those irrelevant operators,  $\epsilon'$  has the lowest dimension and will thus give the largest correction.

The dimension of  $\epsilon'$  is known poorly, because the perturbative series in  $\epsilon$  become more and more divergent and we cannot trust it for  $\epsilon \rightarrow 1$ . Therefore, the estimated dimension of  $\epsilon'$  is even less accurate, let alone the infinite amount of other operators that are present in the theory. That is why only seven operators are being studied at the moment. However, as we present in this paper, these problems do not arise when working with the conformal bootstrap technique. This is because when using the bootstrap, we are not relying on perturbative techniques in a region where perturbation theory breaks down, as is the case for  $\epsilon \rightarrow 1$ .

$T_{\mu\nu}$  is the stress-energy tensor. It does not have an anomalous dimension. It reflects the fact that the Ising model at the critical point is a local theory. Normally,  $T_{\mu\nu}$  puts the theory in a curved background if added to the Lagrangian. For the 3D Ising model this would be difficult to realize in a lab. We can think of it as giving an anisotropy to the spins, for example  $J_x > J_y = J_z$ , which means that spin flips in the  $x$  direction cost more energy than spin flips in the  $y$  or  $z$  direction. This will change the correlation functions in the same way as adding a component of the stress energy tensor to the Lagrangian would. In both cases the theory is no longer isotropic and the presence of a component of  $T_{\mu\nu}$  will break rotational invariance.

$C_{\mu\nu\rho\sigma}$  is a spin-4 operator. It has a very small anomalous dimension, unlike the stress energy tensor. In the free theory  $C_{\mu\nu\rho\sigma}$  is conserved, but this is not the case anymore in the Ising point. Like  $\sigma$ , the anomalous dimension as calculated with the  $\epsilon$ -expansion is second order in  $\epsilon$ . It describes the effect of rotational symmetry breaking. A cubic lattice, on which the Ising model is defined, is not rotationally invariant. However, in the IR, rotational invariance emerges. This is because going to the IR (low energies) is comparable to going to very large length scales. If the length scales are very large, the lattice spacing is relatively small and negligible and you end up in the continuum limit. Lattice effects disappear and rotational invariance emerges. Because we are transferring from no rotational invariance on the cubic lattice in the UV to emergent rotational invariance in the IR, an operator that can break the rotational invariance is needed, otherwise this change cannot take place. The operator that can do this with the lowest dimension is  $C_{\mu\nu\rho\sigma}$ . Since  $C_{\mu\nu\rho\sigma}$  is an irrelevant operator it will vanish in the IR and rotational invariance emerges there, because there is no operator left that can break it (all the other operators have dimensions higher than  $C_{\mu\nu\rho\sigma}$  and will vanish even quicker).

We see that all the operators have nonnegative anomalous dimensions. This is related to reflection positivity or unitarity, which is explained in appendix A.

## 5 Solving the 3D Ising model

In this section we will consider a 3D CFT. We will use a conformal bootstrap to derive a bound on the operator spectrum. To do so we will first introduce the bootstrap condition for the four-point function of the Ising spin operator  $\langle\sigma\sigma\sigma\sigma\rangle$ . Then we will sketch the method that is used to find the bound on the spectrum. To do so we will define a function  $\Lambda$  and let it work on the bootstrap crossing equation. As such it appears that certain dimensions of operators do not obey the condition and therefore can not be included in the spectrum. We show and interpret the results of [19] who used this method.

### 5.1 The conformal bootstrap for $\langle\sigma\sigma\sigma\sigma\rangle$

To examine a 3D CFT, as a first step we will focus on constraints coming from the four-point function of the Ising spin operator  $\langle\sigma\sigma\sigma\sigma\rangle$  that lives in this CFT. The conformal block expansion of this four-point function reads

$$g(u, v) = \sum p_{\Delta, l} G_{\Delta, l}(u, v) \quad (15)$$

where  $p_{\Delta, l} = f_{\Delta, l}^2 \geq 0$  follows from (3) and where the sum runs over all operators that are present in the  $\sigma\sigma$  OPE. This OPE consists of infinitely many operators including the ones listed in Table 1. However, due to Bose symmetry only even spin operators can appear in the OPE. After all, the total spin on the left hand side has to equal that on the right hand side. Contracting two fermionic operators therefore leads to an odd integer spin operator, i.e. a bosonic operator with odd spin. Considering a four point function of four fermionic operators then results in the sum of two odd integers which is always even.

Furthermore, since we're considering a correlation function of four equal operators the four point function must be invariant under the exchange  $1 \longleftrightarrow 3$ . In the configuration where the four operators are located on the corners of a square  $\sigma(x_2)$  is as close to  $\sigma(x_1)$  as  $\sigma(x_4)$  is. Note that we can consider this configuration and still make statements about the general CFT since a CFT does not see length scales such that any configuration is equivalent to this one. As was already explained in section 2.2, in practice the configuration shows that the (12)(34) and (14)(23) channels involve the same OPE coefficients. Therefore, the conformal bootstrap equation takes a rather simple form. Using the expression for the cross-ratios, (4), we see it reduces to

$$v^{\Delta_\sigma} g(u, v) = u^{\Delta_\sigma} g(v, u). \quad (16)$$

Now substituting the conformal block decomposition we get,

$$u^{\Delta_\sigma} - v^{\Delta_\sigma} = \sum' p_{\sigma, l} [v^{\Delta_\sigma} G(u, v) - u^{\Delta_\sigma} G(v, u)], \quad (17)$$

where the left-hand side is the contribution of the unit operator and the sum on the right-hand side runs over all other operators. In [14] this equation has been shown to be a fruitful starting point to extract dynamical information about 2D and 4D CFTs. In the same manner it will be our starting point to examine dynamical information about a 3D CFT.



## 5.2 Method of confining the operator dimension spectrum

To actually confine the spectrum we define  $F_{\Delta,l}^{\Delta\sigma}(u,v) \equiv v^{\Delta\sigma} G_{\Delta,l}(u,v) - u^{\Delta\sigma} G_{\Delta,l}(v,u)$  and rewrite the crossing equation (17),

$$0 = F_{0,0}^{\Delta\sigma}(u,v) + \sum' p_{\sigma,l} F_{\Delta,l}^{\Delta\sigma}(u,v). \quad (18)$$

This is the constraint that is used to confine the spectrum, because only if the right hand side reduces to zero it is possible to describe the 3D CFT in which the four point function  $\langle\sigma\sigma\sigma\sigma\rangle$  appears. To rule out some operator dimensions it suffices to find a linear functional  $\Lambda$  acting on functions of  $(u,v)$  such that,

- $\Lambda(F_{0,0}^{\Delta\sigma}(u,v)) = 1$ , which simply is a normalization condition
- $\Lambda(F_{\Delta,l}^{\Delta\sigma}(u,v)) \geq 0$  for all  $\Delta, l$  in the spectrum

Taking into account the positivity of  $p_{\Delta,l}$ , we see that those spectra for which the above two conditions are true do not obey (18) and therefore cannot describe the 3D CFT we are considering. In practice to produce plots like the ones in Figure 7, 8a, 8c, 8e, 9, for every coordinate in the plane it is checked whether there exists a consistent solution given these two values of operator dimensions of the operators under consideration. For example, if we want to examine the relation between  $\Delta_\sigma$  and  $\Delta_\epsilon$ , for each possible combination  $(\Delta_\sigma, \Delta_\epsilon)$  we check whether there exists a complete spectrum that does not contradict (18). To confine the spectrum even further, we can consider each set  $(\Delta_\sigma, \Delta_\epsilon, \Delta_{\epsilon'})$  and again compare with the crossing equation. Surprisingly enough it is found that just as in 2D CFT,  $\Delta_\epsilon$  is bounded by some function of  $\Delta_\sigma$ ,  $\Delta_\epsilon \leq f(\Delta_\sigma)$ . But before we discuss results we elaborate a bit more on how it can be checked whether the crossing equation is obeyed or not.

Following [19] we consider  $\Lambda$  of the form,

$$\Lambda : F(u,v) \mapsto \sum_{m+2n \leq 2n_{max}+1} \lambda_{m,n} \partial_a^m \partial_b^n F(a,b)|_{a=1,b=0} \quad (19)$$

where  $a, b$  are defined by the relations  $z = (a + \sqrt{b})/2$ ,  $\bar{z} = (a - \sqrt{b})/2$ , where  $\lambda_{m,n}$  are real coefficients and where the range of  $m, n$  depends on the value  $n_{max}$ . Due to the fact that  $F_{\Delta,l}^{\Delta\sigma}(u,v)$  is antisymmetric under the exchange of  $u \longleftrightarrow v$ , only odd  $a$ -derivatives are non-zero. Also, given some  $n_{max}$  there are  $(n_{max} + 1)(n_{max} + 2)/2$  non-zero coefficients  $\lambda_{m,n}$  and the larger you pick  $n_{max}$  the stronger the resulting bound will be, but it will also be computationally more heavy. From the definition of  $F_{\Delta,l}^{\Delta\sigma}(a,b)$  we see that taking derivatives of it comes down to taking derivatives of conformal blocks. So to be able to proceed we need expressions of conformal blocks.

For a long time conformal blocks in 3D (and 4D) were not well understood; they were known only in terms of complicated integrals or power series expansions in  $u, v$ . However, recently progress has been made by [5, 19]. Following their approach in Appendix C we show how from the double power

series expansion introduced in [3],

$$G_{\Delta,0}(u, v) = u^{\Delta/2} \sum_{m,n=0}^{\infty} \frac{[(\Delta/2)_m(\Delta/2)_{m+n}]^2}{m!n!(\Delta+1-\frac{D}{2})_m(\Delta)_{2m+n}} \times u^m(1-v)^n \quad (20)$$

the expressions of the conformal blocks with spin 0 and spin 1,  $G_{\Delta,0}(z)$  and  $G_{\Delta,1}(z)$ , can be obtained. The results are,

$$G_{\Delta,0}(z) = \left(\frac{z^2}{(1-z)}\right)^{\Delta/2} {}_3F_2\left(\frac{\Delta}{2}, \frac{\Delta}{2}, \frac{\Delta}{2} - \alpha; \frac{\Delta+1}{2}, \Delta - \alpha; \frac{z^2}{4(z-1)}\right) \quad (21)$$

$$G_{\Delta,1}(z) = \frac{2-z}{2z} \left(\frac{z^2}{1-z}\right)^{\frac{\Delta+1}{2}} {}_3F_2\left(\frac{\Delta+1}{2}, \frac{\Delta+1}{2}, \frac{\Delta+1}{2} - \alpha; \frac{\Delta}{2} + 1, \Delta - \alpha; \frac{z^2}{4(z-1)}\right). \quad (22)$$

The higher spin conformal blocks can then be calculated by the recursion formula that is derived in Appendix B,

$$\begin{aligned} (l+D-3)(2\Delta+2-D)G_{\Delta,l} &= (D-2)(\Delta+l-1)G_{\Delta,l-2} \\ &+ \frac{2-z}{2z}(2l+D-4)(\Delta-D+2)G_{\Delta+1,l-1} \\ &- \frac{\Delta(2l+D-4)(\Delta+2-D)(\Delta+3-D)(\Delta-l-D+4)^2}{16(\Delta+1-\frac{D}{2})(\Delta-\frac{D}{2}+2)(l-\Delta+D-5)(l-\Delta+D-3)}G_{\Delta+2,l-2}. \end{aligned} \quad (23)$$

This settles the problem of expressing conformal blocks.

In practice in calculating  $\partial_a^m \partial_b^n G_{\Delta,l}$  first  $\partial_a^m G_{\Delta,l}$  up to  $m = 2n_{max} + 1$  is determined. This can be done by using yet another recursion formula. For ease of notation we'll denote  $\partial_a^m \partial_b^n G_{\Delta,l}$  by  $h_{m,n}$ . From (21), (22) and (23) we see that the conformal blocks contain  ${}_3F_2$  hypergeometric functions. Therefore, in order to calculate  $h_{m,0}$  we can make use of the fact that  ${}_3F_2$  hypergeometric functions obey the third order differential equation,

$$(x\hat{D}_{a_1}\hat{D}_{a_2}\hat{D}_{a_3} - \hat{D}_0\hat{D}_{b_1-1}\hat{D}_{b_2-1}){}_3F_2(a_1, a_2, a_3; b_1, b_2; x) = 0, \quad (24)$$

where  $\hat{D}_c \equiv x\partial_x + c$ . From this identity a recursion relation of third order derivatives in terms of second and first order derivatives follows. Taking yet another derivative of the equation yields the fourth order derivative. As such, derivatives up to  $m = 2n_{max} + 1$  can be computed.

Once  $h_{m,0}$  is known,  $h_{m,n}$  in the range  $m+2n \leq 2n_{max} + 1$  follows from the recursion relation that is derived in Appendix D. The result is,

$$\begin{aligned} 2(D+2n-3)h_{m,n} &= 2m(D+2n-3) \\ &\times [-h_{m-1,n} + (m-1)h_{m-2,n} + (m-1)(m-2)h_{m-3,n}] \\ &- h_{m+2,n-1} + (D-m-4n+4)h_{m+1,n-1} \\ &+ [2C_{\Delta,l} + 2D(m+n-1) + m^2 + 8mn - 9m + 4n^2 - 6n + 2]h_{m,n-1} \\ &+ m[D(m-2n+1) + m^2 + 12mn - 15m + 12n^2 - 30n + 20]h_{m-1,n-1} \\ &+ (n-1)[h_{m+2,n-2} - (D-3m-4n+4)h_{m+1,n-2}]. \end{aligned} \quad (25)$$

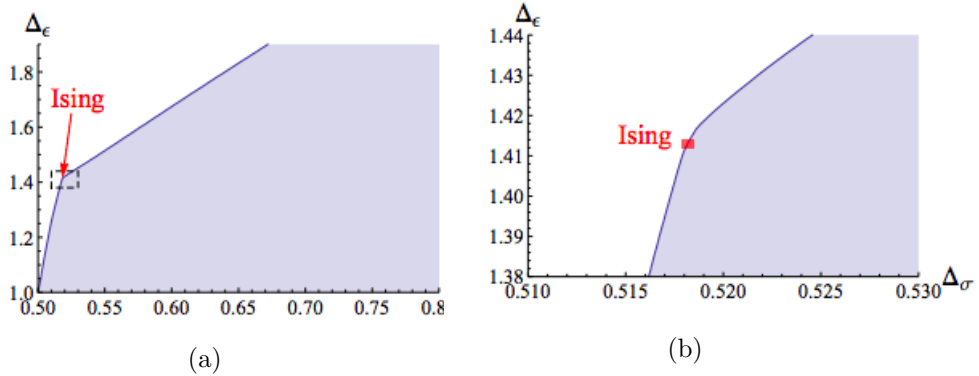


Figure 7: The shaded region is the part of the  $(\Delta_\sigma, \Delta_\epsilon)$  plane that is allowed by the crossing equation (18). Figure (a) shows how the boundary curve starts at the free theory point and then rises. Furthermore, the boundary shows a kink that lies remarkably close to the known 3D Ising model operator dimensions (the tip of the arrow). Figure (b) is the zoom of the dashed rectangle area from Figure (a). The red rectangle is drawn using the  $\Delta_\sigma, \Delta_\epsilon$  error bands given in Table 1. The figures were computed using  $n_{max} = 11$ . Source: [19].

One sees that for example  $h_{m,1}$  can simply be computed by substituting  $h_{m,0}$  and like this all other  $h_{m,n}$  can be determined as well. The problem of confining the spectrum of operators is now reduced to a problem of linear programming which is further explained in [19].

## 5.3 Results

### 5.3.1 Bounds on $\Delta_\epsilon$

The spin field in the four-point function is a zero spin operator,  $l = 0$ , such that from unitarity, (27), we expect  $\Delta_\sigma \geq 0.5$ . If we consider  $\Delta_\sigma$  from this lower bound up until the arbitrarily chosen upper bound,  $0.5 \leq \Delta_\sigma \leq 0.8$ , we can ask the question *what is the maximal allowed  $\Delta_\epsilon$  by (17)?*

This question was answered by [19] using the methods explained in the previous section and their results are shown in Figure 7. Just as [16] shows in the 2D case  $\Delta_\epsilon$  is bounded by some function. Also, again it starts at the free theory point - which one can find by considering the action without interactions - and then rises steadily. What is rather interesting is the fact that also in this plot we see a kink. In the 2D case we have seen that the kink corresponds to the Ising point. For 3D [8] has reported Ising dimensions,

$$\Delta_\sigma = 0.5183(4), \quad \Delta_\epsilon = 1.412(1).$$

Comparing this with the location of the kink we see it's remarkably close to the Ising dimensions in 3D. More specific, the boundary of the allowed region intersects the red rectangle that was drawn using the  $\Delta_\sigma$  and  $\Delta_\epsilon$  error bands.

What can be concluded from this? In order to find values for the operator dimensions conformal invariance was *assumed*. Comparing the results that were found using conformal bootstraps with the operator dimensions that

were found by other techniques, we see that they are not inconsistent: the operator dimensions that were found previously are contained in the shaded region of Figure 8a. Second, almost half of the rectangle  $(\Delta_\sigma, \Delta_\epsilon)$  has been ruled out so it is possible to gain information about 3D CFTs using a bootstrap technique. Furthermore, it seems as if the Ising point lies remarkably close on the boundary of the allowed region, if not on the boundary. However, there is no explanation yet why this should be the case.

### 5.3.2 Bounds on $\Delta_\epsilon$ assuming a gap between $\Delta_\epsilon$ and $\Delta_{\epsilon'}$

Just as we can fix two variables and see if there exists a consistent solution for the operator spectrum, we can consider the situation where we constrain three dimensions and see which region is actually allowed by the bootstrap. Operator dimensions of different operators always have a slightly different value, but in the following we assume a certain gap between the operator dimensions of  $\epsilon$  and  $\epsilon'$ . This has been proposed by [16]. In fact we consider three different constraints:  $\Delta_{\epsilon'} \geq 3, 3.4, 3.8$ . The question we now try to answer is, *assuming an extra constraint, namely  $\Delta_{\epsilon'} \geq x$ , what is the region of the  $(\Delta_\sigma, \Delta_\epsilon)$  plane that is allowed by (17)?*

The first assumption  $\Delta_{\epsilon'} \geq 3$  is chosen since we know that the 3D Ising critical point is reached by fine-tuning just one parameter, the temperature. Because the Ising point lies in the IR, only relevant operators determine the CFT; the irrelevant operators are suppressed. The fact that there is only one parameter to be fine-tuned means that there can be only one relevant  $\mathbb{Z}_2$  even scalar operator and that  $\epsilon', \epsilon''$  etc. must be irrelevant. Given the dimension of the theory that we consider the lowest value of  $\Delta_{\epsilon'}$  that makes sense to describe the region around the Ising point is 3. In Figures 8a, 8b the plot that results from imposing the constraint  $\Delta_{\epsilon'} \geq 3$  is shown. One sees that yet a bigger part of the spectrum is excluded, but that the 3D Ising point is maintained.

When considering the stronger bounds  $\Delta_{\epsilon'} \geq 3.4, 3.8$  for which the results are shown in Figures 8c, 8d and Figures 8e, 8f even larger portions of the operator dimension space gets excluded. The upper branch seems to end at the 3D Ising point whereas the lower one terminates near the free theory.

The zoomed Figures, 8b, 8d, 8f, show that the allowed region barely intersects the 3D Ising point. In fact, the more constrained  $\Delta_{\epsilon'}$  gets, the less the boundary of the shaded region intersects the Ising point rectangle. This has been examined closer by [19]. It was found that the intersection disappeared when  $\Delta_{\epsilon'} \geq 3.840(2)$ . We can therefore conclude that  $3 \leq \Delta_{\epsilon'} \leq 3.840(2)$ .

This conclusion is affirmed when  $\Delta_\epsilon$  is fixed to its maximal value in Fig. 7 and the maximal value of  $\Delta_{\epsilon'}$  is examined. Figure 9 shows the same behaviour as in 2D: a rapid growth around the (3D) Ising value of  $\Delta_\sigma$ . It allows  $\epsilon'$  to quickly become irrelevant in this region (one can see from the figure that  $[\epsilon'] > 3$  just before the Ising point which is indicated by the red vertical line). However, around the 3D Ising  $\Delta_\sigma$  the bound is  $\Delta_{\epsilon'} \lesssim 3.84$  which is consistent with what was found above.

The illuminating part of this story is the fact that the conformal bootstrap

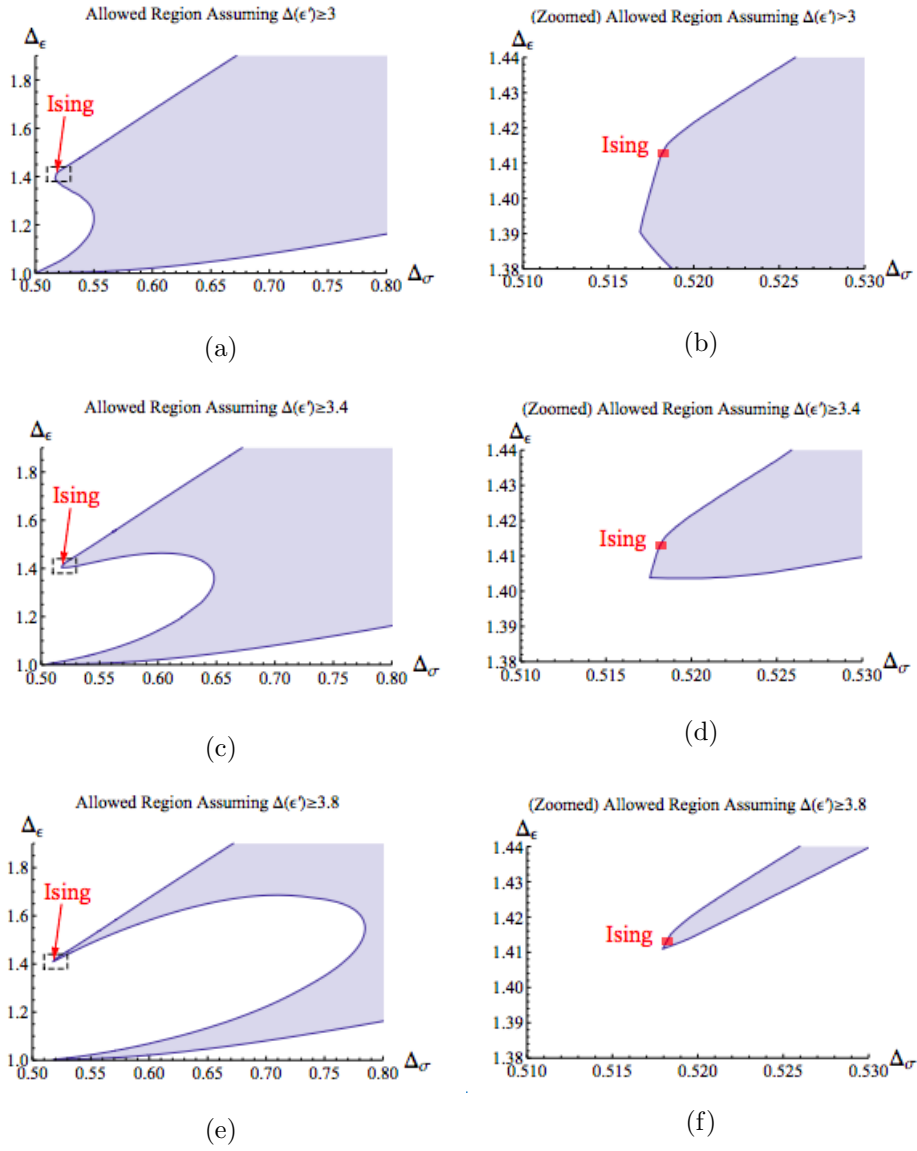


Figure 8: The same figure as Figure 7, but imposing the extra constraint  $\Delta_\epsilon \geq \{3, 3.4, 3.8\}$ . Source: [19].

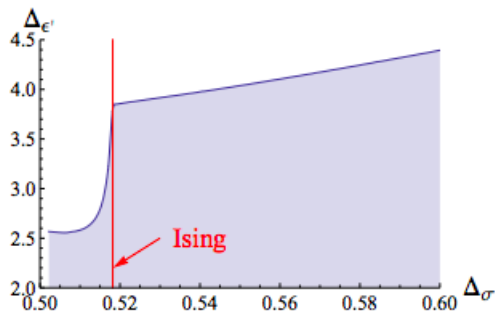


Figure 9: The bound on  $\Delta_{\epsilon'}$  under the condition that  $\Delta_{\epsilon}$  has been fixed to its maximal allowed value by (18). In this plot  $n_{max} = 10$ . The width of the vertical red line marking the 3D Ising value of  $\Delta_{\sigma}$  is about five times the error band in Table 1. Source: [19].

technique shows how operator dimensions depend on each other. From a renormalization group point of view this has not been seen before. When using the  $\epsilon$  expansion for example each operator dimension has to be computed separately. The dependency of dimensions can make it a lot easier to gain the complete spectrum and to describe the complete CFT.

### 5.3.3 Bounds on the gap in the spin 2 sector

The story so far considered the scalar sector of the 3D Ising model. However, it's also interesting to examine the dimensions of operators with non-vanishing spin. The first operator with spin that appears in the  $\sigma \times \sigma$  OPE is the energy stress tensor,  $T_{\mu\nu}$ , which has spin 2 (as can also be seen from Table 1). However, as a first try not  $T_{\mu\nu}$  is considered but the second spin 2 operator in the OPE,  $T'_{\mu\nu}$ .

Figure 10 shows how  $\Delta_{T'}$  is bounded by the crossing symmetry constraint (17). The bound is shown as a function of  $\Delta_{\sigma}$  and falls rapidly around the 3D Ising value of  $\Delta_{\sigma}$  which again has been denoted by the red vertical line. In fact the bound of  $\Delta_{T'}$  shows opposite behaviour to that of  $\Delta_{\epsilon'}$ . It starts at a plateau at  $\Delta_{T'} \sim 5.7$ , then drops around the 3D Ising point to stay at a value around  $\Delta_{T'} \sim 3.5$  as  $\Delta_{\sigma}$  increases. Notable is that assuming a gap of for example  $\Delta_{T'} \geq 4$  leads to a sharp upper bound on  $\Delta_{\sigma}$ . One can see from Figure 10 that if this gap would be assumed, the upper bound on the dimension of  $\sigma$  would be  $\Delta_{\sigma} \leq 0.52$ . Taking into account the Figures 8a, 8c, 8e very small regions in the  $(\Delta_{\sigma}, \Delta_{\epsilon})$  would be obtained.

Unfortunately the operator  $T'_{\mu,\nu}$  hasn't been computed before by other techniques in contrast with the other operators discussed in this paper. Therefore we can not immediately check the results obtained by the bootstrap technique for this operator. [19] justifies why the result that was found is probably correct. [19] also elaborates on the restrictions resulting from the bootstrap on the dimension of higher spin primaries such as  $C_{\mu\nu\kappa\lambda}$  and on

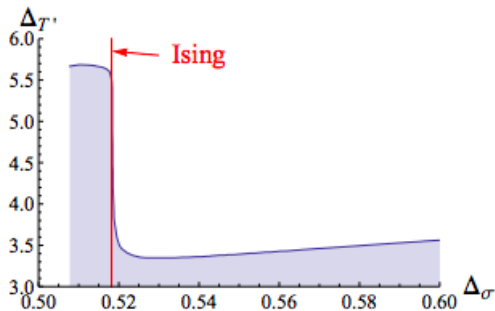


Figure 10: The allowed values for  $\Delta_{T'}$  given the crossing equation (17).  $T'_{\mu\nu}$  is the second spin 2 operator. To obtain these results  $n_{max} = 10$  was used and the 3D Ising vertical line is five times wider than the error band in Table 1. The region of  $\Delta_\sigma$  close to unitarity hasn't been shown due to numerical instabilities. Source: [19].

the bounds on central charges.

## 6 Outlook

In this paper we reviewed recent progress that was made by [19] in solving the CFT describing the 3D Ising model at critical temperature in the continuum limit using the conformal bootstrap technique. Even though it is not well understood why conformal invariance should be a general feature of criticality, it was *assumed* that the 3D Ising critical point is conformal. However, the results that were obtained by using the bootstrap technique are not inconsistent with the values of the 3D Ising operator dimensions that were known before from other techniques (like  $\epsilon$ -expansion, Monte Carlo simulations etc.). This justifies assuming conformal invariance at the 3D Ising point. To further test if the assumption is indeed correct the three-point function  $\langle \sigma(x)\sigma(y)\epsilon(z) \rangle$  on the lattice could be measured experimentally and compared with the functional form that follows from conformal symmetry. The advantage of the conformal bootstrap technique over other methods is that it is far more accurate. In fact, up to some numerical errors that can be made arbitrarily small it is completely rigorous. In series expansions, like  $\epsilon$ - or loop-expansions, for example only the first few terms are computed and the higher ones are neglected all together, even though for example in the  $\epsilon$ -expansion we do not know if we can neglect higher order terms, since  $\epsilon \rightarrow 1$ . In lattice simulations it can be difficult to control the errors induced by discretizing the theory. The conformal bootstrap techniques do not have these problems.

Another advantage is the dependence of operator dimensions on each other. Most of the bounds that were found seem to essentially be saturated by the values realized in the 3D Ising model. This suggests a recursive approach of determining the dimensions: first fix  $\epsilon$  to its maximal dimension, then given this information compute the maximal dimension of  $\epsilon'$ , etc., just as was done to obtain Figure 9. Note moreover that even though we have been focussing

on the 3D case, the results are in fact applicable to all  $D$ .

It is impressive that imposing only the first and simplest bootstrap condition - the one following from the four-point function  $\langle\sigma\sigma\sigma\sigma\rangle$  - excludes such a large region of the space of solutions. Moreover, close to the 3D Ising point the boundary shows a kink. It seems as if the 3D Ising point lies *on* this kink on the boundary. This might have interesting consequences for obtaining some analytical understanding of the 3D Ising model: firstly, the crossing symmetry constraint is expected to allow fewer solutions on the boundary than in the interior, perhaps even a single solution [19]. Secondly, around the kink we have seen that the operator spectrum rapidly rearranges itself (Figure 9, 10). It has been found that such spectrum rearrangements correspond to linear degeneracies among various conformal blocks. Therefore it is important to study this phenomenon in more detail because it brings along the possibility of gaining some analytical understanding of the 3D Ising model.

It would also be interesting to examine bootstrap conditions coming from other correlators since the spectrum might be confined even further. Including  $\langle\sigma\epsilon\sigma\epsilon\rangle$  and  $\langle\epsilon\epsilon\epsilon\epsilon\rangle$  for example would be nice to start with. The former is crossing symmetric in the  $\sigma \times \epsilon$  expansion and as can be seen from (5) the conformal block of  $\sigma$  will appear with the same coefficient  $f_{\sigma\sigma\epsilon}^2$  as the conformal block of  $\epsilon$  in the  $\langle\sigma\sigma\sigma\sigma\rangle$  analysis. The latter correlator is interesting because its expansion involves the same  $\mathbb{Z}_2$ -even operators as  $\langle\sigma\sigma\sigma\sigma\rangle$ .

Overall, the conformal bootstrap technique in  $D > 2$  has shown itself fruitful to examine CFTs. With regards to the 3D Ising model, it hasn't been solved yet, but interesting behaviour and enough future perspective has been revealed.



## Appendix A Some basic Conformal Field Theory

Many books and articles have been written about CFTs and for the reader who is unfamiliar with this topic, this large amount of study material might be overwhelming. Therefore, we included a short summary of some basic CFT knowledge which we used to further build on in the rest of the article. We will discuss the difference between scale invariance, Weyl invariance and conformal invariance. Then we will give all the transformations in the conformal group and the corresponding operators. We will also explain the concept of radial quantization and state-operator correspondence, which is fundamental to CFT. For this appendix, we have mostly taken content from [7, 2, 15].

### A.1 Scale and Weyl invariance

In (Effective) Quantum Field theories (QFTs) running coupling constants show up. This means that the coupling constants related to some interaction term in the Lagrangian take different values at different energy scales. The way these couplings run with the energy scale is determined by the beta function. The beta function differs for each system and can be calculated using the Callan-Symanzik equation,

$$\left[ \mu \partial_\mu + \sum_i \beta \lambda_i \partial_{\lambda_i} - n\gamma \right] \Gamma^{n,m} = 0,$$

where  $\gamma$  is the anomalous dimension,  $\mu$  is the energy scale,  $\lambda$  is the coupling and  $\Gamma^{n,m}$  are the  $n$ -point functions. The zero points of the beta function are called fixed points. At those fixed points the couplings do not change with the energy scale and the theory is said to be scale invariant. The two-point function of two scalar operators  $\mathcal{O}$  (no spin) has the form,

$$\langle \mathcal{O}_1(x) \mathcal{O}_2(y) \rangle \propto \frac{1}{|x - y|^{2\Delta}},$$

where  $\Delta$  is the dimension of the operators. The dimensions of the two operators must be the same. The two-point function must have this form due to translational and scale invariance <sup>1</sup>.

A theory is scale invariant under a scale transformation  $x \rightarrow \lambda x$ , or in the infinitesimal form  $x \rightarrow x + \delta \lambda x$ , if the action satisfies ,

$$S[x, \mathcal{O}_\Delta(x), g_{\mu\nu}] = S[\lambda x, \lambda^{-\Delta} \mathcal{O}_\Delta(x), g_{\mu\nu}] \stackrel{\lambda x \rightarrow x}{=} S[x, \lambda^{f-\Delta} \mathcal{O}_\Delta(x), \lambda^2 g_{\mu\nu}],$$

where  $g_{\mu\nu}$  is the metric and  $f$  denotes the number of indices of the operator  $\mathcal{O}_\Delta$  because this will define how  $\mathcal{O}_\Delta$  will transform under a coordinate transformation,

$$\mathcal{O}'_{\mu\nu\dots}(y) = \frac{\partial x^\alpha}{\partial y^\mu} \frac{\partial x^\beta}{\partial y^\nu} \dots \mathcal{O}_{\alpha\beta\dots}(x).$$

---

<sup>1</sup>See also [2, p. 30-31] for a derivation.

This will lead to the constraint,

$$\delta S = \left\langle \int d^d x T_{\mu\nu} g^{\mu\nu} \sqrt{g} \right\rangle = \left\langle \int d^d x T_{\mu}^{\mu} \sqrt{g} \right\rangle = 0,$$

This constraint reduces to  $T_{\mu}^{\mu} = \partial_{\mu} G^{\mu}$  for some function  $G^{\mu}$  for a flat metric.  $T_{\mu\nu}$  is the energy momentum tensor.

There is another type of ‘symmetry’ called Weyl invariance. It is actually not a real symmetry since it changes the metric, but rather an equivalence. We have a transformation of the form  $g_{\mu\nu}(x) \rightarrow \Omega(x)g_{\mu\nu}(x)$ , or in infinitesimal form,  $g_{\mu\nu}(x) \rightarrow g_{\mu\nu}(x) + \omega(x)g_{\mu\nu}(x)$ . A theory is Weyl invariant if the action obeys,

$$S[x, \mathcal{O}_{\Delta}(x), g_{\mu\nu}] = S[x, \Omega^{-\Delta}(x)\mathcal{O}_{\Delta}(x), \Omega^2(x)g_{\mu\nu}(x)].$$

This leads to the constraint,

$$\delta S = \left\langle \int d^d x \sqrt{g} T_{\mu\nu} g^{\mu\nu} \omega(x) \right\rangle = 0,$$

which will give  $T_{\mu}^{\mu} = 0$ , a traceless energy momentum tensor. It looks very similar to the constraint for scale invariance, but  $\Omega(x)$  is coordinate dependent as opposed to  $\lambda$ , which means that we cannot get rid of the factor  $\Omega^2(x)$  in front of the metric by a coordinate transformation. Therefore, the metric changes non-trivially and we are looking at two different manifolds before and after the transformation. This is also why we cannot really call Weyl invariance a symmetry.

## A.2 Conformal invariance

Conformal invariance can be thought of as somewhere in between scale invariance and Weyl invariance. It has more symmetry than scale invariance, namely also invariance under special conformal transformations as we will see later on, but is less constraining than Weyl invariance, where the stress energy tensor must be traceless and not only a second derivative of some function. A conformal transformation leaves the angle between vectors invariant. It can be defined as a coordinate transformation which acts on the metric as a Weyl transformation [18]. It is a Weyl transformation where we can get rid of the factor  $\Omega^2(x)$  by a coordinate transformation, so we have a diffeomorphism between the two manifolds before and after the transformation. For a general coordinate transformation  $x \rightarrow x'$ , the metric changes under a conformal transformation in such a way that the transformation obeys,

$$g_{\mu\nu}(x)\Lambda(x) = g'_{\mu\nu}(x') = \frac{\partial x'^{\rho}}{\partial x^{\mu}} \frac{\partial x'^{\sigma}}{\partial x^{\nu}} g_{\rho\sigma}(x')$$

The theory is conformally invariant if

$$S[x, \mathcal{O}_{\Delta}(x), g_{\mu\nu}(x)] = S[x', \mathcal{O}'_{\Delta}(x'), g'_{\mu\nu}(f(x'))] = S[x', \mathcal{O}'_{\Delta}(x'), g_{\mu\nu}(x)]$$

We used a Weyl transformation to get the metric back in its original form. From this we get the constraint (this involves some algebra),

$$\delta S = \int d^d x L^{\rho\mu} \partial_\rho \partial_\mu \partial_\nu \varepsilon^\nu$$

Using Noether's theorem this reduces to  $T_\mu^\mu = \partial_\alpha \partial_\beta L^{\alpha\beta}$ , where  $L^{\alpha\beta}$  is some general function. In this expression  $\varepsilon^\mu$  is the conformal vector and can take the forms,

$\varepsilon^\mu = a^\mu$	$a^\mu = cst$	translations
$\varepsilon^\mu = \omega_\nu^\mu x^\nu$	$\omega_\nu^\mu = antisymm$	Lorentz transformations
$\varepsilon^\mu = \lambda x^\mu$	$\lambda = cst$	scale invariance
$\varepsilon^\mu = b^\mu x^2 - 2\chi^\mu b_\nu x^\nu$		special conformal transformations

A theory that is Weyl invariant ( $T_\mu^\mu = 0$ ) is also conformally invariant ( $T_\mu^\mu = \partial_\alpha \partial_\beta L^{\alpha\beta}$ ). This can be seen straight away. It can also be shown that the opposite is true in any dimension: a theory that has conformal symmetry also has Weyl invariance. This can be achieved by redefining the energy momentum tensor. We will not show it here, since it is not of current interest. The relation between scale invariance and conformal invariance however is. In two dimensions – and trivially also in one dimension – Zamolodchov and Polchinski [11, 21] have shown that scale invariance also implies conformal invariance. So far, this has not been proven yet for three dimensions.

Let us go back to the conformal transformations that we found. We can define an operator for each of these transformations which transforms a function  $f(x) \rightarrow f(x) + \mathcal{O}_\varepsilon f(x)$ . The operators are,

$P_\mu = i\partial_\mu$	translations
$M_{\mu\nu} = i(x_\mu \partial_\nu - x_\nu \partial_\mu)$	Lorentz transformations
$D = -ix^\mu \partial_\mu$	scale invariance
$K_\mu = i(x^2 \partial_\mu - 2x_\mu x^\nu \partial_\nu)$	special conformal transformations

We can interpret  $D$  as a Hamiltonian, governing the evolution of states in our theory. Now it is not an evolution in time, as we would get with a normal Hamiltonian, but a dilatation. Furthermore, we can interpret  $P_\mu$  as a raising operator because  $[D, P_\mu] = iP_\mu$  and  $K_\mu$  as a lowering operator because  $[D, K_\mu] = -iK_\mu$ .  $D$  acts on the vacuum and on a state created by  $\mathcal{O}_\Delta$  in the following way,

$$D|0\rangle = 0$$

$$D|\Delta\rangle = D\mathcal{O}_\Delta(0)|0\rangle = [D, \mathcal{O}_\Delta(0)]|0\rangle = i\Delta|\Delta\rangle.$$

Acting with  $D$  on a state gives the dimension of the operator creating that state. We can divide the operators in two classes, primaries and descendants.

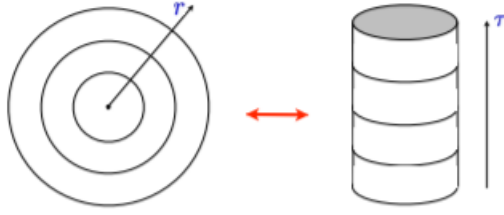


Figure 11: Mapping from  $\mathbb{R}^d$  to  $S^{d-1} \times \mathbb{R}$ . Source: [15]

Primary operators having dimension  $\Delta = h + \bar{h}$ , where  $h$  is the *conformal weight*, transform as follows under a conformal transformation  $z \rightarrow f(z)$ :

$$\mathcal{O}_\Delta(z, \bar{z}) \rightarrow \mathcal{O}'_\Delta(z', \bar{z}') = \left( \frac{\partial f(z)}{\partial z} \right)^h \left( \frac{\partial \bar{f}(\bar{z})}{\partial \bar{z}} \right)^{\bar{h}} \mathcal{O}_\Delta(f(z), \bar{f}(\bar{z}))$$

Note that this equation is written in the language of 2D CFTs, where we have a complex space parametrized by  $z$  and  $\bar{z}$ . However, in 3D, primary operators will transform in the same way under a conformal transformation.

For primary operators,  $[K_\mu, \mathcal{O}_\Delta(0)] = 0$ . Since  $K_\mu$  can be thought of as a lowering operator the primaries are the lowest dimensional operators. The descendants can be found by acting on the primaries with the raising operator  $P_\mu$ ,

$$\mathcal{O}_{\Delta, \mu_1, \dots, \mu_n} = [P_{\mu_1}, \dots [P_{\mu_n}, \mathcal{O}_\Delta] \dots]$$

The spectrum of operator dimensions is bounded from below because  $[K_\mu, \mathcal{O}_\Delta(0)] = 0$  for primary operators, so there exist a lowest value for the dimension of primaries. Descendants are formed by raising the dimension and will thus always have a higher dimension. The dimension of the primary operators must be larger than a certain value, depending on the spin of the operator, to get a unitary (or reflection positive in Euclidean space) theory where all states have nonnegative norms. If the dimension of the primaries is too low, states will have negative norms which is not well-defined. The values are,

$$\Delta \geq \frac{D}{2} - 1 \quad l = 0 \quad (26)$$

$$\Delta \geq l + D - 2 \quad l \neq 0, \quad (27)$$

where  $D$  is the dimension of the theory considered and  $l$  the spin of the operator.

Conformal field theories are usually defined on an infinite space-time cylinder  $\mathbb{R} \times S^{D-1}$ . Time is running from  $-\infty$  to  $\infty$  along the long axis of the cylinder and space is compactified on  $S^{d-1}$  with the coordinate  $x$  running from 0 to  $L$  and  $(0, t) = (L, t)$ . Because the space is now compactified, the spectrum of the theory will be quantized. We can map the cylinder to the (complex) plane (see Figure 11) where we will have concentric circles with a radius that is

growing with time.  $\tau = -\infty$  is mapped to the origin of the concentric circles and  $\tau = \infty$  lies infinitely far away. This process is called radial quantization. Since  $D$  acts as a Hamiltonian and the evolution of a state (now living on the circumference of the cylinder) is given by  $e^{iD\tau} |\Delta\rangle = e^{i\Delta\tau} |\Delta\rangle$ , the spectrum that is quantized is the spectrum of dimensions of operators. Now we can think of states as created by primary operators inserted at the origin [7],

$$|\Delta\rangle = \lim_{x \rightarrow 0} \mathcal{O}_\Delta(0) |0\rangle.$$

Those states have well defined dimension  $\Delta$  and are annihilated by  $K_\mu$ . We can also think of this the other way around. For states with a well defined dimension  $\Delta$  that are annihilated by  $K_\mu$ , we can construct a local primary operator  $\mathcal{O}_\Delta$  which we can insert at the origin to create this state. The fact that we can do this both ways is called the *state-operator correspondence*.

## Appendix B Recursion relations for conformal blocks

Using the same functions as [5] do we write the conformal blocks as,

$$G_{\Delta,l} = F_{\lambda_1,\lambda_2}, \quad \lambda_1 = \frac{1}{2}(\Delta + l), \quad \lambda_2 = \frac{1}{2}(\Delta - l) \quad (28)$$

Next to this we introduce the functions,

$$\beta_p \equiv \frac{p^2}{4(2p-1)(2p+1)}, \quad (29)$$

$$\begin{aligned} \mathcal{F}_0 &\equiv \frac{1}{z} + \frac{1}{\bar{z}} - 1 \\ \mathcal{F}_1 &\equiv (1-z)\partial_z + (1-\bar{z})\partial_{\bar{z}} \\ \mathcal{F}_2 &\equiv \frac{z-\bar{z}}{z\bar{z}}(D_z - D_{\bar{z}}), \quad \text{where } D_z \equiv z^2(1-z)\partial_z^2 - z^2\partial_z \end{aligned} \quad (30)$$

It was shown in [5] that  $\mathcal{F}_i F_{\lambda_1,\lambda_2}$  can be written as linear combinations of  $F_{\lambda'_1,\lambda'_2}$ . Following [19] we can write,

$$\begin{aligned} \mathcal{F}_0 F_{\lambda_1,\lambda_2} &= \frac{l+2\alpha}{l+\alpha} F_{\lambda_1,\lambda_2-1} + \frac{l}{l+\alpha} F_{\lambda_1-1,\lambda_2} \\ &+ \frac{(\Delta-1)(\Delta-2\alpha)}{(\Delta-1-\alpha)(\Delta-\alpha)} \left( \frac{l+2\alpha}{l+\alpha} \beta_{\lambda_1} F_{\lambda_1+1,\lambda_2} + \frac{l}{l+\alpha} \beta_{\lambda_2-\alpha} F_{\lambda_1,\lambda_2+1} \right) \end{aligned} \quad (31)$$

$$\begin{aligned} \mathcal{F}_1 F_{\lambda_1,\lambda_2} &= \frac{l+2\alpha}{l+\alpha} F_{\lambda_1,\lambda_2-1} + \frac{l}{l+\alpha} (\lambda_1 + \alpha) F_{\lambda_1-1,\lambda_2} \\ &+ \frac{(\Delta-1)(\Delta-2\alpha)}{(\Delta-1-\alpha)(\Delta-\alpha)} \left( \frac{l+2\alpha}{l+\alpha} (-\lambda_1 + \alpha + 1) \beta_{\lambda_1} F_{\lambda_1+1,\lambda_2} \right. \\ &\left. + \frac{l}{l+\alpha} (\lambda_2 + 2\alpha + 1) \beta_{\lambda_2-\alpha} F_{\lambda_1,\lambda_2+1} \right) \end{aligned} \quad (32)$$

$$\begin{aligned} \mathcal{F}_2 F_{\lambda_1,\lambda_2} &= (\Delta-1) \frac{l(l+2\alpha)}{l+\alpha} [F_{\lambda_1,\lambda_2-1} - F_{\lambda_1-1,\lambda_2}] \\ &- \frac{(\Delta-2\alpha)(\Delta-1-2\alpha)}{(\Delta-1-\alpha)(\Delta-\alpha)} (\beta_{\lambda_1} F_{\lambda_1+1,\lambda_2} - \beta_{\lambda_2-\alpha} F_{\lambda_1,\lambda_2+1}) \end{aligned} \quad (33)$$

In order to find a recursion relation we can combine two equations, say  $\mathcal{F}_0$  and  $\mathcal{F}_2$ , to eliminate one of the terms  $F_{\lambda'_1, \lambda'_2}$ . Say we eliminate  $F_{\lambda_1+1, \lambda_2}$ . To do so we compute a linear combination of  $\mathcal{F}$  and  $\mathcal{F}_2$ . It gives us,

$$\begin{aligned} \frac{1}{2}[(\Delta - 1 - 2\alpha)\mathcal{F}_0 + \frac{\mathcal{F}_2}{l}]F_{\lambda_1, \lambda_2} &= (\Delta - 1 - \alpha)\frac{l + 2\alpha}{l + \alpha}F_{\lambda_1, \lambda_2-1} - \frac{\alpha(\Delta + l - 1)}{l + \alpha}F_{\lambda_1-1, \lambda_2} \\ &+ \frac{(\Delta - 1)(\Delta - 2\alpha)(\Delta - 1 - 2\alpha)}{(\Delta - 1 - \alpha)(\Delta - \alpha)}\beta_{\lambda_2-\alpha}F_{\lambda_1, \lambda_2+1} \end{aligned} \quad (34)$$

Shifting the spin,  $l = l - 1$ , and noticing this is equivalent to shifting  $\lambda_2 = \lambda_2 + 1$  such that  $\Delta = \Delta + 1$  we can write this expression in terms of the conformal blocks again as,

$$\begin{aligned} \frac{(\Delta - \alpha)(l + 2\alpha - 1)}{l + \alpha - 1}G_{\Delta, l} &= \frac{\alpha(\Delta + l - 1)}{l + \alpha - 1}G_{\Delta, l-2} + \frac{1}{2}[(\Delta - 2\alpha)\mathcal{F}_0 + \frac{\mathcal{F}_2}{l-1}]G_{\Delta+1, l-1} \\ &- \frac{\Delta(\Delta - 2\alpha)(\Delta - 2\alpha + 1)}{(\Delta - \alpha)(\Delta - \alpha + 1)}\beta_{\frac{1}{2}(\Delta - l + 2 - 2\alpha)}G_{\Delta+2, l-2} \end{aligned} \quad (35)$$

However, as  $z = \bar{z}$  – which is the case we’re interested in – we see from (30) that  $\mathcal{F}_2$  vanishes. Writing  $\alpha = D/2 - 1$  again and multiplying both sides by  $2(l + \alpha - 1)$  we’re left with the non-derivative recursion relation,

$$\begin{aligned} (l + D - 3)(2\Delta + 2 - D)G_{\Delta, l} &= (D - 2)(\Delta + l - 1)G_{\Delta, l-2} \\ &+ \frac{2 - z}{2z}(2l + D - 4)(\Delta - D + 2)G_{\Delta+1, l-1} \\ &- \frac{\Delta(2l + D - 4)(\Delta + 2 - D)(\Delta + 3 - D)(\Delta - l - D + 4)^2}{16(\Delta + 1 - \frac{D}{2})(\Delta - \frac{D}{2} + 2)(l - \Delta + D - 5)(l - \Delta + D - 3)}G_{\Delta+2, l-2} \end{aligned} \quad (36)$$

Note that this relation is especially useful along the line  $z = \bar{z}$  and that it can be used to compute high spin conformal blocks efficiently. However, we need two conformal blocks as input to be able to do calculations, whereas we only have one available, namely  $G_{\Delta, 0}$ . Luckily we can consider a different combination of functions, that of  $\mathcal{F}_0$  and  $\mathcal{F}_1$ , and find a recursion relation for which only one block is needed. We use this relation to find  $G_{\Delta, 1}$  from  $G_{\Delta, 0}$  in Appendix C but then calculate all higher spin blocks using (36).

To find the recursion relation resulting from combining  $\mathcal{F}_0$  and  $\mathcal{F}_1$ , or (31) and (32), the same logic as before is applied. After first computing  $(\mathcal{F}_1 + (\lambda_1 - \alpha - 1)\mathcal{F}_0)F_{\lambda_1, \lambda_2}$  to eliminate  $F_{\lambda_1+1, \lambda_2}$  again, then shifting the spin in the same way, i.e.  $l = l - 1$ ,  $\lambda_2 = \lambda_2 + 1$ ,  $\Delta = \Delta + 1$ , and passing to the  $G_{\Delta, l}$  notation, we get:

$$\begin{aligned} \frac{(\Delta - \alpha)(l + 2\alpha - 1)}{(l + \alpha - 1)}G_{\Delta, l} &= \left(\frac{1}{2}(\Delta + l - 2\alpha - 2)\mathcal{F}_0 + \mathcal{F}_1\right)G_{\Delta+1, l-1} \\ &- (l - 1)\left(\frac{\Delta(\Delta - 2\alpha + 1)}{(\Delta - \alpha)(\Delta - \alpha + 1)}\beta_{\frac{1}{2}(\Delta - l + 2 - 2\alpha)}G_{\Delta+2, l-2} + \frac{\Delta + l - 1}{l + \alpha - 1}G_{\Delta, l-2}\right) \end{aligned} \quad (37)$$

One can see directly that it can be used to compute  $G_{\Delta,1}$  since the last two terms vanish in this case.

## Appendix C Conformal blocks of spin 0 and 1

According to [19] for scalar exchange ( $l = 0$ ) conformal blocks have a double power series representation,

$$G_{\Delta,0}(u, v) = u^{\Delta/2} \sum_{m,n=0}^{\infty} \frac{[(\Delta/2)_m(\Delta/2)_{m+n}]^2}{m!n!(\Delta + 1 - \frac{D}{2})_m(\Delta)_{2m+n}} \times u^m(1-v)^n \quad (38)$$

Here  $(q)_n$  is the rising Pochhammer symbol which is defined as,

$$(q)_n = \begin{cases} 1 & n = 0 \\ q(q+1)\cdots(q+n-1) & n > 0 \end{cases} \quad (39)$$

From this definition we can see that  $(\Delta/2)_{m+n} = (\Delta/2)_m(m + \Delta/2)_n$  and likewise that  $(\Delta)_{2m+n} = (\Delta)_{2m}(2m + \Delta)_n$ . Therefore, using the power series expansion of the hypergeometric function,

$${}_2F_1(a, b; c; z) = \sum_{n=0}^{\infty} \frac{(a)_n(b)_n z^n}{(c)_n n!}, \quad (40)$$

we can rewrite (38) as,

$$G_{\Delta,0}(u, v) = \sum_{m=0}^{\infty} \frac{((\Delta/2)_m)^4}{m!(\Delta - \alpha)_m(\Delta)_{2m}} u^{\frac{\Delta}{2}+m} \times {}_2F_1\left(m + \frac{\Delta}{2}, m + \frac{\Delta}{2}; 2m + \Delta; 1 - v\right) \quad (41)$$

where  $\alpha = D/2 - 1$  now.

Now we use the integral representation of  ${}_2F_1$ ,

$${}_2F_1(a, b; c; z) = \frac{\Gamma(c)}{\Gamma(b)\Gamma(c-b)} \int_0^1 dt \frac{t^{b-1}(1-t)^{c-b-1}}{(1-tx)^a}. \quad (42)$$

Substituting it in (41) we see,

$$\begin{aligned} G_{\Delta,0}(u, v) &= \sum_{m=0}^{\infty} \frac{((\Delta/2)_m)^4}{m!(\Delta - \alpha)_m(\Delta)_{2m}} u^{\frac{\Delta}{2}+m} \\ &\quad \times \frac{\Gamma(2m + \Delta)}{\Gamma(m + \frac{\Delta}{2})\Gamma(m + \frac{\Delta}{2})} \int_0^1 dt \frac{t^{m+\frac{\Delta}{2}-1}(1-t)^{m+\frac{\Delta}{2}-1}}{(1-tx)^{m+\frac{\Delta}{2}}} \\ &= \frac{\Gamma(\Delta)}{\Gamma(\frac{\Delta}{2})^2} \int_0^1 \frac{dt}{t(1-t)} \left( \frac{(1-t)tu}{1-t(1-v)} \right)^{\Delta/2} \\ &\quad \times \sum_{n=0}^{\infty} \frac{(\frac{\Delta}{2})_n(\frac{\Delta}{2})_n}{n!(\Delta - \alpha)_n} \left( \frac{(1-t)tu}{1-t(1-v)} \right)^n \\ &= \frac{\Gamma(\Delta)}{\Gamma(\frac{\Delta}{2})^2} \int_0^1 \frac{dt}{t(1-t)} X^{\Delta/2} {}_2F_1\left(\frac{\Delta}{2}, \frac{\Delta}{2}; \Delta - \alpha; X\right). \end{aligned} \quad (43)$$

In the second step we used that since  $\Gamma(z) = \frac{\Gamma(z+n+1)}{z(z+1)\cdots(z+n)}$ , we have that  $\Gamma(\Delta) = \frac{\Gamma(\Delta+2m)}{(\Delta)_{2m}}$  and  $\frac{1}{\Gamma(\Delta/2)} = \frac{(\Delta/2)_m}{\Gamma(m+\Delta/2)}$ . In the last step we simply defined the variable,

$$X = \frac{(1-t)tu}{1-t(1-v)}. \quad (44)$$

Now let us use the hypergeometric identity,

$${}_2F_1(a, b; c; z) = (1-x)^{-b} {}_2F_1(c-a, b; c; \frac{z}{z-1}) \quad (45)$$

and the fact that from a powerserie point of view the hypergeometric function is symmetric under the exchange of  $a$  and  $b$ . Then we can write,

$$G_{\Delta,0}(u, v) = \frac{\Gamma(\Delta)}{\Gamma(\frac{\Delta}{2})^2} \int_0^1 \frac{dt}{t(1-t)} Y^{\Delta/2} {}_2F_1\left(\frac{\Delta}{2}, \frac{\Delta}{2} - \alpha; \Delta - \alpha; -Y\right), \quad (46)$$

$$\text{where } Y = \frac{X}{1-X} = \frac{t(1-t)z\bar{z}}{(1-tz)(1-t\bar{z})}.$$

Now we can replace  ${}_2F_1$  by its powerseries expansion and integrate the series term by term. Since we're only interested in the case  $z = \bar{z}$  this becomes even simpler. Using Mathematica to calculate the integrals, [19] claims to find,

$$G_{\Delta,0}|_{z=\bar{z}} = \left(\frac{z^2}{1-z}\right)^{\Delta/2} \sum_{n=0}^{\infty} \frac{[(\Delta/2)_n]^3 (\Delta/2 - \alpha)_n}{n! (\Delta)_{2n} (\Delta - \alpha)_n} \left(\frac{z^2}{z-1}\right)^n. \quad (47)$$

Now using the series expansion of  ${}_3F_2$ ,

$${}_3F_2(a_1, a_2, a_3; b_1, b_2; z) = \sum_{n=0}^{\infty} \frac{(a_1)_n (a_2)_n (a_3)_n}{(b_1)_n (b_2)_n} \frac{z^n}{n!}, \quad (48)$$

we can write (47) as,

$$\boxed{G_{\Delta,0}(z) = \left(\frac{z^2}{(1-z)}\right)^{\Delta/2} {}_3F_2\left(\frac{\Delta}{2}, \frac{\Delta}{2}, \frac{\Delta}{2} - \alpha; \frac{\Delta+1}{2}, \Delta - \alpha; \frac{z^2}{4(z-1)}\right)} \quad (49)$$

Here we used that  $\frac{(\Delta/2)_n}{(\Delta)_{2n}} = \frac{1}{4^n} \frac{1}{(\frac{\Delta+1}{2})_n}$ . Equation (49) is the expression that we use to describe the spin 0 conformal block along the line  $z = \bar{z}$ .

It also helps us to find an expression for the spin 1 conformal block,  $G_{\Delta,1}$ , along the  $z = \bar{z}$  line. To do so, we use the recursion relation (37) derived in Appendix B which for  $l = 1$  it reduces to,

$$G_{\Delta,1}(z) = \frac{1}{2(\Delta - \alpha)} \left(\frac{1}{2}(\Delta - 2\alpha - 1)\mathcal{F}_0 + \mathcal{F}_1\right) G_{\Delta+1,0}(z)$$



Substituting the expression for the zero spin conformal block for  $\Delta = \Delta + 1$  and the ones for  $\mathcal{F}_0$  and  $\mathcal{F}_1$  one sees that after making a (partly) change of variables of  $z \mapsto y \equiv \frac{z^2}{4(z-1)}$  which is done for ease of notation the expression for the spin 1 conformal block  $G_{\Delta,1}$  comes down to,

$$G_{\Delta,1}(z) = \frac{2-z}{2(\Delta-\alpha)z} \left( \frac{z^2}{1-z} \right)^{\frac{\Delta+1}{2}} [y\partial_y + \Delta - \alpha]f(y) \quad (50)$$

The function  $f(y)$  is simply the hypergeometric function appearing in the expression for  $G_{\Delta+1,0}$ . Now using the identity for hypergeometric functions,

$$[y\partial_y + b_2 - 1]{}_3F_2(a_1, a_2, a_3; b_1, b_2; y) = (b_2 - 1){}_3F_2(a_1, a_2, a_3; b_1, b_2 - 1; y) \quad (51)$$

we find the final expression for the spin 1 conformal block,

$$G_{\Delta,1}(z) = \frac{2-z}{2z} \left( \frac{z^2}{1-z} \right)^{\frac{\Delta+1}{2}} {}_3F_2 \left( \frac{\Delta+1}{2}, \frac{\Delta+1}{2}, \frac{\Delta+1}{2} - \alpha; \frac{\Delta}{2} + 1, \Delta - \alpha; \frac{z^2}{4(z-1)} \right). \quad (52)$$

## Appendix D Recursion relation $h_{m,n}$

As justified in [19, 4] we use that conformal blocks satisfy a second-order differential equation,

$$\mathcal{D}G_{\Delta,l}(z, \bar{z}) = \frac{1}{2}C_{\Delta,l}G_{\Delta,l}(z, \bar{z}), \quad (53)$$

where  $C_{\Delta,l} \equiv \Delta(\Delta - D) + l(l + D - 2)$  and

$$\mathcal{D} \equiv (1-z)z^2\partial_z^2 - \left( z^2 - (D-2)\frac{z\bar{z}(1-z)}{z-\bar{z}} \right) \partial_z + (z \leftrightarrow \bar{z}). \quad (54)$$

Making a change of variables  $z = (a + \sqrt{b})/2$ ,  $\bar{z} = (a - \sqrt{b})/2$  the last expression takes the form,

$$\begin{aligned} \mathcal{D} &= (2-a)a^2 \left[ \frac{1}{2}(D-1)\partial_b + b\partial_b^2 \right] \\ &+ (2-3a)b^2\partial_b^2 + \left[ \frac{1}{2}(D-9)a - a(3a-4)\partial_a - D + 3 \right] b\partial_b - \frac{1}{4}Da^2\partial_a \\ &+ \frac{1}{4}(2-a)a^2\partial_a^2 - b^2\partial_a\partial_b + \left[ \frac{1}{4}(D-4)\partial_a + \frac{1}{4}(2-3a)\partial_a^2 \right] b \end{aligned} \quad (55)$$

To deduce a recursion relation to calculate  $h_{m,n}$  we apply  $\partial_a^m \partial_b^n$  on (53) where obviously  $\mathcal{D}$  takes the form as in (55). Note that since we're considering the point  $z = \bar{z} = \frac{1}{2}$  we can set  $a$  and  $b$  to  $a = 1, b = 0$ . After shifting  $n \mapsto n - 1$  we find,

$$\begin{aligned} 2(D+2n-3)h_{m,n} &= 2m(D+2n-3) \\ &\times [-h_{m-1,n} + (m-1)h_{m-2,n} + (m-1)(m-2)h_{m-3,n}] \\ &- h_{m+2,n-1} + (D-m-4n+4)h_{m+1,n-1} \\ &+ [2C_{\Delta,l} + 2D(m+n-1) + m^2 + 8mn - 9m + 4n^2 - 6n + 2]h_{m,n-1} \\ &+ m[D(m-2n+1) + m^2 + 12mn - 15m + 12n^2 - 30n + 20]h_{m-1,n-1} \\ &+ (n-1)[h_{m+2,n-2} - (D-3m-4n+4)h_{m+1,n-2}]. \end{aligned} \quad (56)$$

## References

- [1] A.A. Belavin, A.M. Polyakov and A.B. Zamolodchikov, *Infinite conformal symmetry in two-dimensional quantum field theory*, Nuclear Physics B241 (1984), 333–380.
- [2] Ralph Blumenhagen, Erik Plauschinn, *Introduction to Conformal Field Theory With Applications to String Theory*, Lect. Notes Phys. 779 (2009), 1-256
- [3] F. Dolan and H. Osborn, *Conformal four point functions and the operator product expansion*, Nucl.Phys. B599 (2001), 459–496, arXiv:hep-th/0011040 [hep-th].
- [4] F. Dolan and H. Osborn, *Conformal partial waves and the operator product expansion*, Nucl.Phys. B678 (2004) 491–507, arXiv:hep-th/0309180 [hep-th].
- [5] F. Dolan and H. Osborn, *Conformal Partial Waves: Further Mathematical Results*, 2012.
- [6] David Simmons-Duffin, *TASI Lectures on the Conformal Bootstrap* (2016), arXiv: 1602.07982v1 [hep-th]
- [7] Philippe di Francesco, Pierre Mathieu, David Sénéchal, *Conformal Field Theory* (1996), Springer.
- [8] M. Hasenbusch, K. Pinn, S. Vinti, *Critical Exponents of the 3D Ising Universality Class. From Finite Size Scaling With Standard and Improved Actions*, arXiv:hep-lat/9806012.
- [9] Victor Kac, *Contravariant form for infinite dimensional Lie algebras and superalgebras*, Lecture Notes in Physics 94 (1979), 441-445.
- [10] David Poland, David Simmons-Duffin, *The Conformal Bootstrap*, Nature Physics **12** (2016), 535–539.
- [11] J. Polchinski, *Scale and conformal invariance in quantum field theory*, Nucl. Phys. B 303 (1988), 226.
- [12] A.M. Polyakov, *Conformal symmetry of critical fluctuations*, ZhETF Pis. Red. **12**, No. 11 (1970), 538–541.
- [13] A.M. Polyakov, *Non-Hamiltonian approach to conformal quantum field theory*, Zh. Eksp. Teor. Fiz. **66** (1974), 23–42.
- [14] R. Rattazzi, V. S. Rychkov, E. Tonni, and A. Vichi, *Bounding scalar operator dimensions in 4D CFT*, JHEP 12 (2008) 031, arXiv:0807.0004 [hep-th].
- [15] S. Rychkov, *EPFL Lectures on Conformal Field theory*
- [16] S. Rychkov, *Conformal Bootstrap in Three Dimensions?*, arXiv:1111.2115[hep-th].

- [17] S. Rychkov, *The 3D Ising Model and Conformal Bootstrap* (Powerpoint slides, video recording), CERN Winter School on Supergravity, Strings and Gauge Theory, <https://indico.cern.ch/event/183290/contributions/318659/>
- [18] A.N. Schellekens, *Conformal Field Theory*, (2016), Notes of the september 1995 lectures at Saalburg, <https://www.nikhef.nl/t58/CFT.pdf>
- [19] S. El-Showk, M.F. Paulos, D. Poland, S. Rychkov, D. Simmons-Duffin, A. Vichi, *Solving the 3D Ising model with the conformal bootstrap*, Phys. Rev. D 86, 025022, 2012.
- [20] Natalie Wolchover, *Physicists Uncover Geometric ‘Theory Space’*, Quantamagazine, <https://www.quantamagazine.org/using-the-bootstrap-physicists-uncover-geometry-of-theory-space-20170223/>
- [21] A. B. Zamolodchikov, “Irreversibility” of the flux of the renormalization group in a 2D field theory, JETP Lett. 43 (1986) 730 [Pisma Zh. Eksp. Teor. Fiz. 43 (1986) 565]